ANALYSIS OF CANDIDATE COCAINE AND AMPHETAMINE REGULATED TRANSCRIPT (CART) GENES: CHANGES IN ERK PHOSPHORYLATION IN N2a CELLS

A THESIS SUBMITTED TO
THE GRADUATE SCHOOL OF NATURAL AND APPLIED SCIENCES
OF
MIDDLE EAST TECHNICAL UNIVERSITY

BY

AYLA ÖZKILIÇ

IN PARTIAL FULFILLMENT OF THE REQUIREMENTS
FOR
THE DEGREE OF MASTER OF SCIENCE
IN
MOLECULAR BIOLOGY AND GENETICS

JANUARY 2019

Approval of the thesis:

ANALYSIS OF CANDIDATE COCAINE AND AMPHETAMINE REGULATED TRANSCRIPT (CART) RECEPTOR GENES: CHANGES IN ERK PHOSPHORYLATION IN N2a CELLS

submitted by **AYLA ÖZKILIÇ** in partial fulfillment of the requirements for the degree of **Master of Science in Molecular Biology and Genetics Department, Middle East Technical University** by,

Prof. Dr. Halil Kalıpçılar
Dean, Graduate School of **Natural and Applied Sciences** _____

Prof. Dr. Orhan Adalı
Head of Department, **Biological Sciences Dept., METU** _____

Assoc. Prof. Dr. Tülin Yanık
Supervisor, **Biological Sciences Dept, METU** _____

Assoc. Prof. Dr. Çağdaş D. Son
Co-Supervisor, **Biological Sciences Dept, METU** _____

Examining Committee Members:

Prof. Dr. Fatih İzgü
Biological Sciences Department, METU _____

Assoc. Prof. Dr. Tülin Yanık
Biological Sciences Department, METU _____

Assoc. Prof. Dr. Çağdaş D. Son
Biological Sciences Department, METU _____

Assist. Prof. Dr. Erkan Kiriş
Biological Sciences Department, METU _____

Assist. Prof. Dr. Fatima Aerts Kaya
Dept. of Stem Cell Sci., Grad. School of Health Sci., Hacettepe Univ. _____

Date: 16.01.2019

I hereby declare that all information in this document has been obtained and presented in accordance with academic rules and ethical conduct. I also declare that, as required by these rules and conduct, I have fully cited and referenced all material and results that are not original to this work.

Name, Surname: Ayla Özkılıç

Signature:

ABSTRACT

ANALYSIS OF CANDIDATE COCAINE AND AMPHETAMINE REGULATED TRANSCRIPT (CART) RECEPTOR GENES: CHANGES IN ERK PHOSPHORYLATION IN N2a CELLS

Özkılıç, Ayla
M.Sc, Department of Molecular Biology and Genetics
Supervisor: Assoc. Prof. Dr. Tülin Yanık
Co-Supervisor: Assoc. Prof. Dr. Çağdaş D. Son

January 2019, 95 pages

CART is widely expressed in both the central and peripheral nervous system. It encodes CART peptides (CART 55-102 and CART 62-102) that are neurotransmitters and hormones and are positively modulated by leptin which is a satiety hormone. These neuropeptides have important roles in controlling feeding behavior, metabolic rate, hyperphagy, obesity and type 2 diabetes, drug reward, bone remodeling, sensory processing, neuroendocrine function, stress, anxiety, cardiovascular function, gastrointestinal development. Despite the importance of CART, its receptor has not been discovered yet. To understand molecular and cellular pathways of CART, identification of the CART receptor has a high priority.

Studies related to binding of CART showed that CART 55-102 induced dose and time dependent activation of extracellular signal-regulated kinase (ERK) 1 and 2. Moreover, inhibition of CART 55-102 by genistein and pertussis toxin indicated that the upstream kinases MEK1 and 2 were involved the signaling pathway. Therefore, a role for the Gi/Go coupled G protein coupled receptor (GPCR) in CART 55-102 signaling was considered.

Microarray studies were used to analyze over a thousand GPCR signaling related gene products. Among which, 7 candidate genes that may be a CART receptors were determined. In this study, we aimed to express these 7 different candidate CART receptor genes into N2a cells (mouse neuroblastoma cells), stimulate them with CART 62-102 and analyze ERK 1 and 2 phosphorylation (p-ERK) using Western Blot. We hypothesized that candidate gene/s might increase p-ERK in presence of a candidate CART receptor.

The results show that p-ERK 1/2 signaling has not been detected when the cells were transfected with 7 candidate genes. In conclusion, further investigations are needed to be performed to confirm possibility of these genes candidacy as a potential CART receptor.

Keywords: CART, CART receptor candidates, ERK phosphorylation, G Protein Coupled Receptors

ÖZ

ADAY KOKAİN VE AMFETAMİN İLE REGÜLE EDİLEN TRANSKRİPT (CART) RESEPTÖR GENLERİNİN ANALİZİ: N2a HÜCRELERİNDE ERK FOSFORİLASYONUNDAKİ DEĞİŞİMLER

Özkılıç, Ayla
Yüksek Lisans, Moleküler Biyoloji ve Genetik Bölümü
Tez Danışmanı: Doç. Dr. Tülin Yanık
Ortak Tez Danışmanı: Doç.Dr. Çağdaş D. Son

Ocak 2019, 95 sayfa

CART merkezi ve çevresel sinir sisteminde yaygın olarak eksprese edilen, sinir ileticileri ve tokluk hormonu olan leptin ile pozitif olarak regüle edilen hormonlar olarak bilinen CART peptidlerini (CART 55-102 and CART 62-102) kodlayan gendir. Bu nöropeptidler beslenme davranışını, metabolik hızı, aşırı yeme isteğini (hiperfaji), obesiteyi, tip 2 diyabeti, ödül mekanizmasını, kemiklerin yeniden biçimlenmesini, algısal süreci, stres ve endişeyi, kardiyovasküler fonksiyonu, sindirim sistemi gelişmesini kontrol etmekte önemli görevlere sahiptir. CART'ın önemli olmasına rağmen, onun reseptörleri henüz keşfedilememiştir. CART'ın moleküler ve hücresel yolaklarını anlamak için CART reseptörlerinin tanımlanması yüksek önceliğe ve öneme sahiptir.

CART bağlanmasıyla ilgili yapılan çalışmalarda, CART 55-102'nin hücre dışı sinyal ile regule edilen kinaz (ERK) 1 ve 2' nin doz ve zamana bağlı aktivasyonunu indüklediği tespit edilmiştir. Ayrıca, CART 55-102'ın genistein ve pertussis toksin tarafından engellenmesi bir sonraki basamakta olan MEK1 and 2 kinazlarının sinyal yolağına dahil olduğunu göstermiştir. Bu nedenle, CART 55-102 sinyalinde Gi/Go'a bağlı G protein kenetli reseptörün (GPKR) rolü olduğu düşünülmektedir.

Mikrodizi çalışmaları binlerce GPKR gen ürününü analiz etmek için kullanılmıştır. İncelenen genlerin arasından CART reseptör gen/genleri olabilecek 7 gen adayı belirlenmiştir. Bu çalışmada, farklı 7 CART aday reseptör genini N2a hücrelerinde (fare nöroblastoma hücreleri) express etmeyi ve onları CART 62-102 ile uyarıp, Western Blot ile ERK 1 ve 2 fosforilasyonunu (p-ERK) analiz etmeyi amaçlıyoruz. Hipotezimize göre, aday reseptör gen veya genleri CART varlığında N2a hücrelerinde p-ERK'i artırabilir.

Sonuçlarımıza göre, hücreler 7 aday gen ile transfekte edildiği zaman p-ERK 1/2 sinyali saptanamamıştır. Bu genleri olası CART reseptör adayları olarak doğrulamak için daha fazla araştırma yapılmasına ihtiyaç duyulmaktadır.

Anahtar Kelimeler: CART, CART aday reseptörleri, ERK fosforilasyonu, G protein kenetli reseptörler

Dedicated to my beloved family and friends.

ACKNOWLEDGMENTS

I would like to thank to my advisor Assoc. Prof. Dr. Tülin Yanık. She always took care of me and my experiments, thus I cope with all problems and obstacles with her guidance and thoughts. I am grateful to be her student.

Next, I would like to thank to Assoc. Prof. Dr. Çağdaş D. Son for his warm welcome and his many support to me during my experiments and for his insights and criticisms about my research topic.

I also want to thank my thesis committee members; Prof. Dr. Fatih İzgü, Assist. Prof. Dr. Erkan Kiriş and Assist. Prof. Dr. Fatima Aerts Kaya for their contributions to my thesis defence and their valuable thoughts and criticisms.

Finally, thanks to the students of the Yanık laboratory and Ali Akyol, who have helped me during my experiments. Last but not least, I would not accomplish my endeavors without my beloved family and friends endless support and advices.

TABLE OF CONTENTS

ABSTRACT v

ÖZ vii

ACKNOWLEDGMENTS x

TABLE OF CONTENTS xxi

LIST OF TABLES xiv

LIST OF FIGURES xv

LIST OF ABBREVIATIONS xvi

CHAPTERS

1. INTRODUCTION 1

1.1. CART 1

1.2. CART FUNCTIONS 5

1.2.1. CART and Body Weight 5

1.2.2. CART and Peripheral System Functions 8

1.2.3. CART and Psychostimulants 10

1.2.4. CART and Cognitive Functions 12

1.3. CART INDUCED SIGNALING AND BINDING STUDIES 14

1.4. HYPOTHESIS AND AIM 20

1.4.1. Hypothesis 20

1.4.2. Aim 20

2. MATERIALS AND METHODS 21

2.1. Verification of Candidate CART Receptor Genes In Plasmids 21

2.1.1. Streak Plate of Bacterial Cells and Colony Selection..... 21

2.1.2. Plasmid Isolation Protocol 22

2.1.3. Restriction Digestion Reaction of Candidate Genes…….23

2.1.4. Agarose Gel Electrophoresis of Digested Genes……..23

2.1.5. Primer Design for *SCTR*……24

2.1.6. PCR for SCTR Genes……24

2.1.7. Agarose Gel Electrophoresis of SCTR Genes……...25

2.1.8. Colonies Selection…….25

2.1.9. Next Generation Sequencing of *SCTR*…….…….25

2.1.10. Primer Design for TANGO Vector…….……26

2.1.11. PCR for 7 Candidate Genes with TANGO Primers……...26

2.1.12. Sanger Sequencing of GLP1R and GLP2R Genes…….26

2.2. Cell Culture Studies……26

2.2.1. Cell Passaging…….....27

2.2.2. Total Protein Isolation of HEK 293 and N2a Cells……...27

2.2.3. Bradford Assay Protocol……...28

2.2.4. Primary Antibody Verification with Dot Blot……...29

2.2.5. Transfection of N2a Cells with TANGO Vectors…….29

2.2.6. CART Peptide Stimulation of Transfected N2A Cells…… 30

2.3. Western Blot Assay……..30

3. RESULTS 33

3.1. Verification of 7 Candidate CART Receptor Genes In TANGO Vectors...33

3.2. Selection of New Primers for TANGO Vector……35

3.3. Dot Blot Analysis……36

3.4. Western Blot Analysis……..37

4. DISCUSSION 41

5. CONCLUSIONS 45

REFERENCES.....47

APPENDICES

A. Nanodrop Results For Plasmid DNAs 61

B. Tables of Materials For PCR……...63

C. Complete Cell Medium Protocol……67

D. Total Protein Concentrations of Cells (µg/µl)……69

E. Tables of Materials For Western Blot……..71

F. p-ERK 1/2 Western Blot Protocol……..79

G. Verification of 7 Candidate CART Receptor Genes In TANGO Vectors…..83

LIST OF TABLES

TABLES

Table 1. Preparation of Diluted Albumin (BSA) Standarts 28

LIST OF FIGURES

FIGURES

Figure 1. Rat proCART and CART 55-102 structure 2
Figure 2. Human prepro-CART 3
Figure 3. Comparison of human and rat CART preprohormone 3
Figure 4. CART localization in the brain regions 4
Figure 5.Activation of p-ERK in PC12, CATH.a, N2a, HEK293, GH3 and AtT20 cells 16
Figure 6. Effects of genistein, pertussis toxin and U0126 on CART stimulated p-ERK in AtT20 cells.....17
Figure 7. Dose–response graph for p- ERK1/2 in AtT20 cells……..17
Figure 8. Proposed CART receptor signaling……....18
Figure 9. Agarose Gel Image of PCR for 7 Candidate CART Receptor Genes……35
Figure 10. Dot Blot Imaging……..37
Figure 11. Western Blot Image of 5 minutes CART stimulated N2a ……...38
Figure 12: Western Blot Image of 10 minutes CART stimulated N2a …….39

LIST OF ABBREVIATIONS

ABBREVIATIONS

ACTH	Adrenocorticotropic hormone
AD	Alzheimer's Disease
APS	Amonium persulfate
Arc	Arcuate nucleus
AtT-20	Mouse pituitary epithelial-like tumor cell line
BDNF	Brain derived neurotrophic factor
BMI	Body mass index
cAMP	Cyclic adenosine monophosphate
CART	Cocaine and Amphetamine Regulated Transcript
CART-LI	CART like immunoreactivity
CARTPT	CART gene
CASR	Calcium sensing receptor
CathII.a	Mouse catecholaminergic cell line
CREB	CAMP responsive element binding protein
CRF	Corticotropin-releasing hormone
CSF	Cerebrospinal fluid
DA	Dopamine
DMN	Default mode network
EGR-1	Early growth response 1
ERK	Extracellular signal regulated kinase
GBM	Glioblastoma

GCs	Granulosa cells
GH3	Rat pituitary derived cell line
Glp1r	Glucagon like peptide 1 receptor
Glp2r	Glucagon like peptide 2 receptor
GPCR	G protein coupled receptor
Gpr133	G-protein coupled receptor 133
Gpr116	G-protein coupled receptor 116
Grm1	Glutamate metabotropic receptor 1
HEK293	Human embriyonic kidney cell line
HEPG2	Human liver cancer cell line
HPA axis	Hypothalamic pituitary adrenal axis
HPT	Hypothalamic pituitary thyroid axis
icv	Intracerebroventricularly
ih	Intrahippocampal
ip	Intraperitoneal
Leu	Leucine amino acid
LH	Lateral hypothalamus
LMA	Locomotor activity
MEK	Mitogen activated protein kinase (MAPK) kinase
mRNA	Messenger RNA
N2a	Mouse neuroblastoma cell line
NAc	Nucleus accumbens
NMDA	N-methyl-D-aspartate receptor

NPY	Neuropeptide Y
NRF2/HO-1	Nuclear factor erythroid 2-related factor heme oxygenase-1
NTS	Nucleus of the solitary tract
ORF	Open reading frame
PACAP	Pituitary adenylate cyclase activating protein
PAGE	Polyacrylamide gel electrophoresis
PC12	Rat adrenal gland pheochromocytoma cell line
p-CREB	Phosphorylated CREB
PD	Parkinson's Disease
PVN	Paraventricular nucleus
RANKL	Receptor activator of nuclear factor-κB ligand
SCTR	Secretin receptor
SDS	Sodium dodecyl sulfate
TEMED	Tetramethylethylenediamine
TetR	Tetracycline controlled transactivator
TRH	Thyrotropin-releasing hormone
TRK	Tyrosine receptor kinase
TSH	Thyroid stimulating hormone
VMN	Ventromedial hypothalamic nucleus
VTA	Ventral tagmental area

CHAPTER 1

INTRODUCTION

1.1. CART

Cocaine and amphetamine regulated transcript was discovered as a specific mRNA in rat stratium brain region. Its levels increase when cocaine and amphetamine are injected into the stratium. Therefore, this transcript was called "cocaine and amphetamine-regulated transcript" (CART). It was later understood that CART mRNA produces CART prepropeptides (CARTPT) which are proteolytically cleavaged into smaller and active forms (Douglas et al., 1995). Isolated CART peptides from rat tissues showed that there are two different active CART peptides called CART 55–102 and CART 62–102 (Tim et al., 1999). The structures of these active peptides are similar in human and rats (Douglas et al., 1995). In the rat, two alternatively spliced mRNAs are also translated into a long peptide of 102 amino acids (aa) and a short peptide of 89 aa (Figure 1).

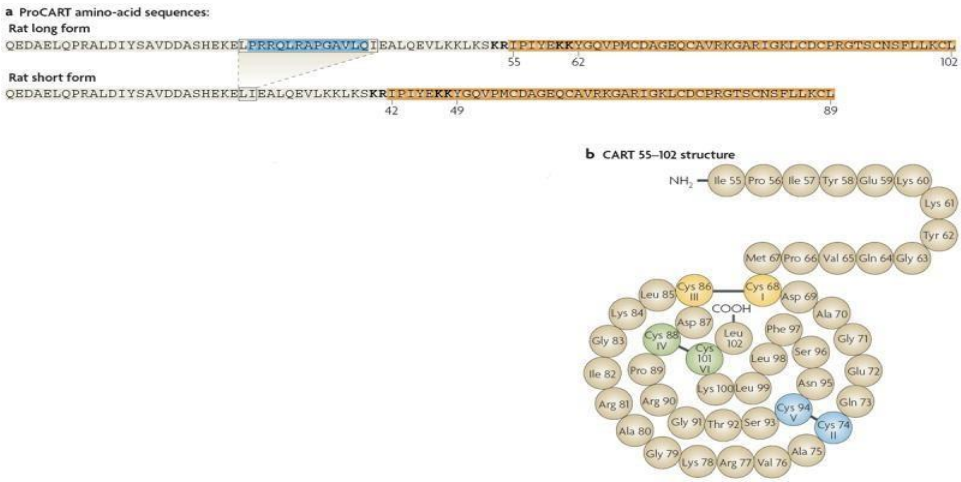

Figure 1: Rat proCART and CART 55-102 structure. A) Two splice variants of CART mRNA **B)** The rat CART 55–102 aa structure (Kuhar et al., 2008).

In humans, *CARTPT* is localized on chromosome 5 and is almost 2,5 kb. The transcript of the gene is 933 bp long and has 3 exons. *CARTPT* has two alternatively spliced mRNAs which produce a 129 aa long peptide and 116 aa short peptide (Kuhar et al., 2002). The proCART peptide has 89 aa. Active CART peptides are CART 42–89 and CART 49–89 and these peptides have the same aa sequence (Figure 2). There is a slight difference between human proCART and rat proCART. Aa 42 is an isoleucine in the rat peptide but a valine in the human peptide (Thim et al., 1998; Stein et al., 2006) (Figure 3).

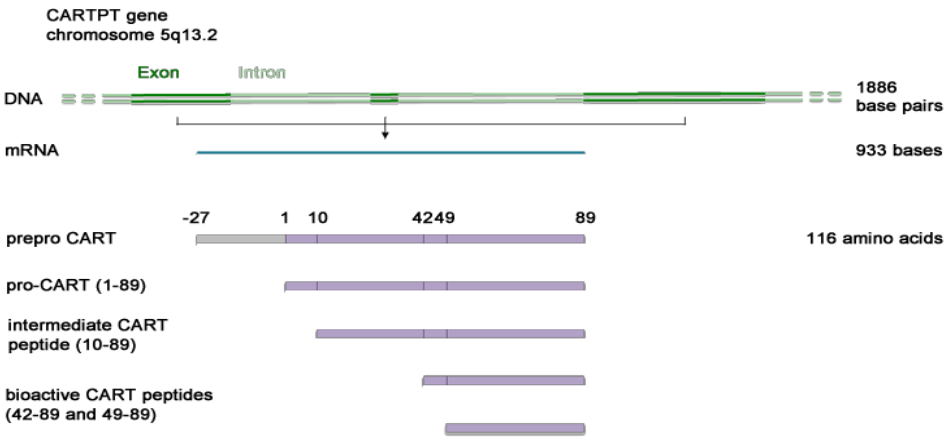

Figure 2: Human prepro-CART. It is a 116 aa peptide. The short form of the peptide is 89 aa peptide (CART 28-116) and it has two active peptides (CART 42-89 and CART 49-89) (Douglass et al., 1995).

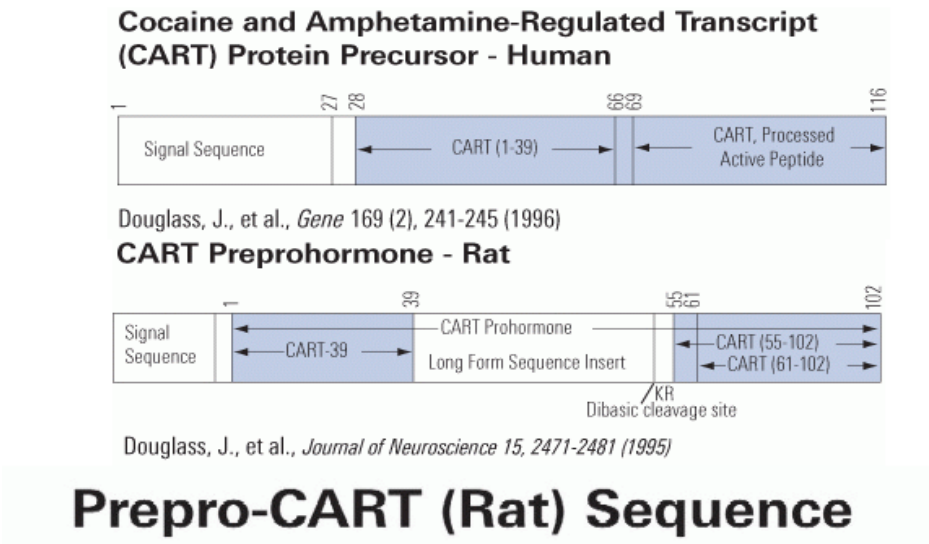

Figure 3: Comparison of human and rat CART preprohormone (Douglass et al., 1995).

CART peptides are found mainly in the central nervous system and the peripheral nervous system. In the central nervous system, they are distributed in multiple brain regions, including the dopaminergic system; Ventral Tagmental Area (VTA) and Nucleus Accumbens (NAc), hypothalamus, pituitary, hindbrain (Figure 4). In the peripheral nervous system, they are found in adrenal glands, pancreas, liver, ovarian, esophageal enteric nervous system, sympathetic neurons, the gastrointestinal tract and its enteric nervous system (Koylu et al., 1997; Vicentic et al., 2007).

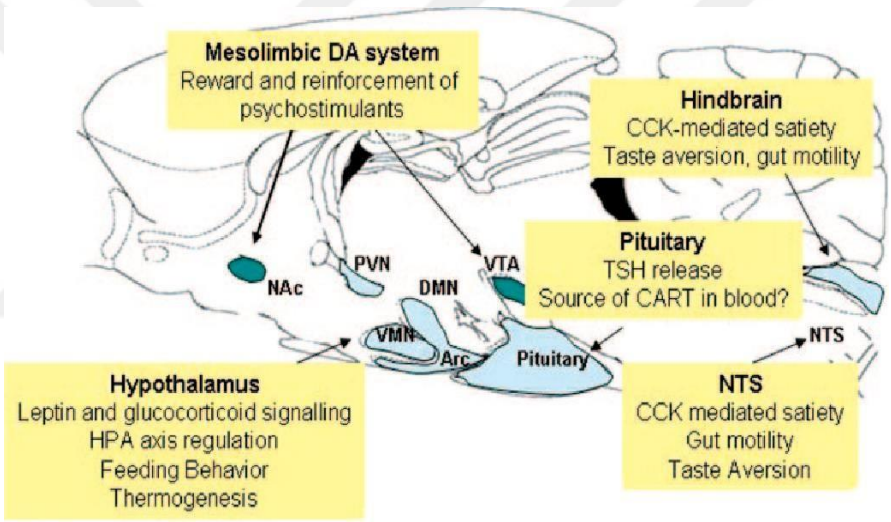

Figure 4: CART localization in the brain regions. The four regions are the dopaminergic system (Ventral Tagmental Area (VTA) and (Nucleus Accumbens) NAc), hypothalamus; Paraventricular Nucleus (PVN), Default Mode Network (DMN), Ventromedial Hypothalamic Nucleus (VMN) and Arcuate Nucleus (Arc), pituitary and hindbrain; Nucleus of the Solitary Tract (NTS) (Vicentic et al., 2007).

1.2. CART FUNCTIONS

CART peptides were found to have many functions in the body. CART functions are related with food intake, reward, addiction, bone remodeling, sensory processing, the stress response, anxiety, depression, cardiovascular function and gastrointestinal motility. It is also thought to be involved in type 2 diabetes, obesity, hyperphagia, Alzheimer's disease and Parkinson's disease (Douglas et al., 1995; Tim et al., 1999).

1.2.1. CART and Body Weight

CART expression can be detected in brain regions that are related to feeding (Elmquist et al., 1999). Feeding control regions are VMN, Lateral Hypothalamus (LH), Arc, PVN, NTS (Koylu et al., 1998) and the NAc (Smith et al., 1999). In the PVN, hormones that regulate feeding are thyrotropin-releasing hormone (TRH) (Broberger et al., 1999) and corticotropin releasing factor (CRF) (Sarkar et al., 2004). Pituitary hormone secretion and energy metabolism are also regulated in the PVN. Moreover, CART interacts with neuropeptide Y (NPY) and is positively regulated by leptin which are both important regulators of feeding (Lambert et al., 1998).

Leptin activates the CART's gene promoter and transducer (Dominguez et al., 2002). Thus, CART inhibits food intake. Besides leptin, CART activity is affected by many other regulators in the brain. Recently, RANKL was found be related with feeding and metabolism. When RANKL was injected to the mice by centrally, the CART levels were increased and NPY levels were decreased. It was stated that RANKL decreases food intake and feeding by affecting the CART and NPY neurons (Zhu et al., 2018).

To investigate the effect of CART on feeding, many studies were carried out. It was shown that feeding was decreased significantly by intracerebroventricularly (icv) administration of CART peptide into the rat brain (Lambert et al., 1998). Feeding and weight gain were decreased by central administration of CART in lean and obese animals (Larsen et al., 2000). In addition, insulin and leptin levels were

decreased with CART given by icv (Rohner-Jeanrenaud et al., 2002). Feeding was decreased when CART peptide was given into the NAc (Yang et al., 2005). However, food intake was increased when CART was injected into different hypothalamic regions. This effect was followed with dramatic inhibition of feeding after 4 hours to a day post-injection of CART. Therefore, CART was thought to decrease feeding and show anorectic action (Abbott et al., 2001). Moreover, another study showed that c-fos expression in the PVN was stimulated with CART and corticosterone secretion was increased. Thus, feeding was inhibited (Larsen et al., 2000) and CART levels even further increased (Vicentic et al., 2006).

CART produced in peripheral areas is also associated with feeding. It is expressed in islet cells and is increased in diabetic rat cells, demonstrating that they regulate islet hormone production (Wierup et al., 2006). Islet hormone production was stimulated by affecting the beta cells *in-vitro* and cell death was inhibited by CART (Wierup et al., 2006; Sathanoori et al., 2013). By regulating hormone production, CART can decrease feeding. In another study, body weight of *CARTPT* knockout mice increased and glucose removal by cells was impaired and insulin secretion was decreased (Wierup et al., 2006). Peripheral CART levels were affected with presence or absence of fuel. During fasting, CART blood levels were changed and its daily rhythm was disrupted. Moreover, TSH and tyroid gland hormon levels were decreased after fasting (García-Luna et al., 2017).

Inhibitory effect of CART on feeding was also investigated in obese mice. In obese mice with nonfunctional leptin receptors, CART levels were increased by leptin reinforcement (Kristensen et al., 1998) and body weight was decreased by leptin administration (Ahima et al., 1998). In high-fat diet induced obese mice, CART levels are decreased because of a defect in leptin receptors (Tian et al., 2004). In anorexia, a condition resulting from nonfunctional leptin signaling, CART levels are reduced. Therefore, it was concluded that CART inhibitory effects are mediated through leptin and its receptor. Leptin related studies were also carried out for obesity. Mice with hyperleptinemia became obese and showed increased CART

levels (Tsuruta et al., 2002). CART mRNA in the hypothalamus was increased in mice fed with a high-fat diet. Lipid stores and fat concentration were decreased and the amount of leptin was increased. Body fat accumulation was decreased with CART neuron activity and its catabolic actions (Wortley et al., 2004).

The effect of CART on human obesity was examined in an Italian family. The cause of the obesity was a missense mutation in *CARTPT*. Because of the mutation, Leu was replaced with Phe and resulting in severe obesity in the family (del Giudice et al., 2001). Generation of same mutation in AtT20 (mouse pituitary cells) cells resulted in decrease CART levels (Dominguez et al., 2004, Yanik et al., 2006). CART levels and brain derived neurotropic factors (BDNF) were examined in obese patients underwent a gastric bypass. CART levels were initially increased, this effect was diminished at the end of one year. Meanwhile, BDNF levels were decreased directly after surgery. Since it is known that CART and BDNF are associated with feeding, it is possible that they may serve as biomarkers to monitor the effects of gastric surgery short term (Muñoz-Rodríguez et al., 2018).

The effect of CART on feeding can be regulated by chemicals and hormones. Estradiol inhibits food intake, as shown in a study where estradiol was injected to ovariectomized (OVX) rats to generate estrous-phase conditions resulting in decreased feeding when compared to the OVX control mice (Butera 2010). CART was also given with intracerebroventricularly (icv) way to the rats that treated with estradiol. Feeding was further decreased after CART intake. Therefore, CART induced reduction of feeding can be increased by estradiol administration (Silva et al., 2010). This study showed that hypothalamic CART may be affected by estradiol. Reduction of food intake with the lack of estradiol may be CART mediated (Dandekar et al., 2012).

1.2.2. CART and Peripheral System Functions

CART is expressed in islet cells of the pancreas. Since it is known that insulin production is regulated by glucose, GLP-1-stimulated insulin secretion was examined and it was shown that insulin can be increased by CART. Ca^{+2} oscillations that release insulin from the beta cells were promoted by CART. In addition, glucagon production was decreased by CART, not just in mouse islets, but also in human islets by affecting the alpha cells. During hyperglycemia, CART mRNA was increased in beta cells and this condition could be prevented by insulin administration. These studies demonstrated that CART regulates islet cell hormone production in human and mice islets. Therefore, this may be a potential therapeutic target for diabetes and obesity (Abels et al., 2016).

CART is also expressed in ovaria. Ovarian CART expression was first reported in the bovine ovary (Yao et al., 2004) and ovarian CART expression was associated with unhealthy follicle formation. CART also was shown to be a negative regulator of FSH and an inhibitor of follicular estradiol production *in-vivo* (Folger et al., 2009). CART was also expressed in the ovarian granulosa cells (GCs) of obese mice fed with high-fat diet. CART expression in GCs was promoted by leptin. Aromatase mRNA expression and steroidogenesis were inhibited by CART. Since CART mRNA expression in GCs and protein levels in follicular fluids are proportionally related with body mass index (BMI) in women, high BMI induces CART expression in the ovary and negatively affects ovarian functions (Ma et al., 2016). Therefore, central obesity and disturbations of hypothalamic-pituitary-ovarian axis are generally linked with anovulatory infertility (Zain et al., 2008) and hyperleptinemia. Effects of elevated leptin levels are thought to be mediated by CART expression in the ovary. Likewise, the effect of leptin on Kiss1 neurons is modulated by CART neuron activity in the Arc nucleus. CART and Kiss1 mRNA expression were increased in female mice fed with a short term high fat diet. Thus, the effect of leptin was increased by elevated CART levels induced by the diet. Thus, Kiss1 expression was

increased indirectly by CART and induced in early puberty in female mice (Venancio et al., 2017).

The effects of CART peptide on other peripheral systems were also investigated. CART 55-102 was injected into the rabbit brain by icv, arterial pressure and kidney sympathetic nerve activity were increased by CART in a dose dependent way. Epinephrine, norepinephrine, glucose levels, insulin, vasopressin and cortisol levels were increased too. These results showed that icv injected human CART 55–102 has a role in the nervous system and induces adrenal hormones in the body. Moreover, icv administration of CART was shown to increase plasma corticosterone and oxytocin concentrations. Thus, the CART peptide can affect the HPA axis. Leptin was also given to animals by icv resulting in activation of adrenal system and increased arterial pressure. It was thought that these effects were activated by CART. After CART was given to hypertensive obese mice, blood pressure decreased. Therefore, this is considered to be a control mechanism for homeostasis, especially for the cardiovascular and sympathetic system (Romeu et al., 2018; Matsumura et al., 2000).

The effects of CART on the enteric nervous system was investigated and showed that CART-like immunoreactive (CART-LI) neurons were found in porcine esophagus fragments. CART was also found in association with acetylcholine transporter and nitrergic neurons in these fragments. These results showed that CART may modulate esophageal functions in the enteric nervous system (Makowska et al., 2018). CART-LI was also detected in porcine small intestine. Acrylamide was given to the pigs in a gelatin capsule and after exposure, fragments of small intestine were examined for CART activity. CART levels were increased in neurons of intestine in response to the toxic effects of acrylamide. Thus, CART is considered a safeguard against neuronal toxins in the gut (Palus et al., 2018).

1.2.3. CART and Psychostimulants

Many studies demonstrated that CART can regulate the reward mechanism and serve as a psychostimulant. It was known that CART transcripts and its peptides are localized in reward linked brain regions (NAc and VTA in the mesolimbic dopaminergic system) and these neurons are associated with dopamine (DA) and gamma-aminobutyric acid (GABA) neurons that are the sites of drug addiction (Dallvechia-Adams et al., 2002). Experiments indicated that CART is expressed in neurons where the effects of psychostimulants exert their actions.

The association between drug reward, CART and the dopaminergic system was determined by various studies. CART and DA receptor mRNAs were found in the same brain regions (Jones et al., 2006). These studies also explored how the dopaminergic system exerts its effect on CART neurons. By increasing the CREB level, CART gene expression was regulated by DA (Tang et al., 2003). CART peptide levels, CREB levels and cAMP were increased in neurons of cocaine addicted victims. Moreover, DA activity was changed by CART by stimulating the DA neurons or by inhibiting the DA neurons. Therefore, the relationship between CART peptide, DA and GABA in terms of psychostimulatory effects were later on proven using anatomical and behavioral studies (Tang et al., 2003).

CART also influences behavioral effects of psychostimulants. After CART was injected to the rat VTA after cocaine administration, locomotor activity (LMA) was increased (Kimmel et al., 2000). This activity was prevented using the DA receptor antagonist haloperidol, suggesting that the dopaminergic system and CART peptide work together (Jaworski et al., 2003). Likewise, increased CART in the NAc was seen after regular exposure to cocaine (Mattson et al., 2005). Moreover, in the amygdala and cortex region of the brain, CART mRNA was increased after cocaine exposure. In CART knockout (KO) mice, the responses to amphetamine and cocaine were decreased in comparison to control animals (Couceyro et al., 2005). These mice showed less locomotor activity in response to CART. This study demonstrated

that reinforcing behavioral effects of psychostimulants are regulated by CART.

CART has been shown to have effects on drugs and their rewarding properties. For example; opiates, such as morphine are related to dopamine, GABA and glutamate (Koob et al., 2005; Pierce et al., 2006). Morphine withdrawal can affect CART levels (Upadhya et al., 2012, Bakhtazad et al., 2016); CART levels in the CSF were increased after high doses of morphine. However, CART levels were decreased in addicted rats (Daly et al., 1996). Here, the motivation for reward was decreased and during withdrawal, CART levels were increased (Bakhtazad et al., 2016). When male Wistar rats were injected with morphine, CART mRNA and peptide levels decreased. However, when a high dose of morphine was used, CART mRNA and peptide levels increased in CSF. Therefore, CART appears to reduce the reinforcing effects of opioids (Bakhtazad et al, 2017). CART peptide levels can also be regulated by alcohol and nicotine. A mutation in the *CARTPT* was linked with DA receptor-sensitivity in the Korean population (Jung et al., 2004) and it was found that CART levels were further increased after alcohol intake in this population (Salinas et al., 2006; Vicentic et al., 2006). In other study, it was discovered that the dopamine signal transduction system is also controlled by nicotinic receptors. Nicotinic receptors and dopamine producing neurons are stimulated after nicotine intake. Dopamine is secreted after nicotine intake and leads to increasing movements in the animals. Locomotor activities were further increased by additional CART administration (Janhunen et al., 2004; Koylu et al., 2016).

CART peptides are known to localize in brain parts related to depression, anxiety and stress and studies showed that stress conditions and increased cAMP can regulate psychostimulants by changing the CART mRNA and peptide levels (Vicentic et al., 2006). In a study, where depression was induced in mice by isolating them socially and CART peptide was given by icv, the severity of depression in the animals decreased gradually. When animals were forced to swim, movements of the animals injected with CART were increased, whereas their immobile time was decreased. These results suggested that CART works likely as an antidepressant

(Jaworski et al., 2008).

Production of adrenocorticotropin hormone (ACTH) is induced by CRF from the pituitary brain region and causes adrenal glands to produce glucocorticoids. CART levels are adjusted and increased by glucocorticoids, whereas stress conditions decrease CART and glucocorticoids (Holsboer et al., 2008). Vrang and his team detected that CART can induce oxytocin secretion from the hypothalamus (Vrang et al., 1999). Since oxytocin can reduce depression like behavior, it can regulate the HPA-axis and CART is thought to have antidepressant properties (Job et al., 2011).

The HPT axis also affects depression by including the thyroid gland hormones and TRH. This hormone is known for its antidepressant properties (Szuba et al., 2005) and it was demonstrated that peptide levels of TRH are increased by CART activity. Moreover, CART and the TRH system show synergistic effects and inhibit dopamine release from the hypothalamus (Job et al., 2011). BDNF also decreases depression like altitudes (De Foubert et al., 2004; Hendolin et al., 2003) and BDNF expression can be increased by CART in neuronal cells. Furthermore, when serotonin levels are increased, it was observed that depression is decreased and serotonergic neurons are regulated by CART (Ma et al., 2007). Therefore, it is thought that CART may have antidepressant properties by regulating other hormones and peptides (Job et al., 2011).

1.2.4. CART and Cognitive Functions

CART is distributed in the cortical regions and hippocampus. In these regions, the Ca^{2+} influx is modulated by CART through membrane proteins and used to develop learning and memory skills (Upadhya et al., 2011; Jin et al., 2015).

Neurons can be protected from cell death due to lack of oxygen and glucose by CART by the activating ERK 1/ 2 in the AtT20 cells (Vicentic et al., 2006; Rogge et al., 2008). Memory can be developed by hyperphosphorylation of ERK. These

studies indicated that synaptic plasticity and memory formation are regulated by ERK (Kelly et al., 2003). In a recent study, rats were treated with CART-antibody by icv and intrahippocampal (ih) injections and with NMDA antagonist intraperitoneally (ip). After that, rats explored the novel objects in less time according to controls. After treatment with CART, novel object exploration developed. Thus, CART may support recognition memory and these processes are modulated by NMDA receptors in the hippocampus (Ashish et al., 2016).

The effect of CART was also analyzed using a transgenic mice model of Alzheimer Disease (AD) and a protective effect of CART on neurons was observed. When transgenic mice were treated with CART, memory deficits, synaptic structure and long-term potentiation was fixed, however, the Aβ plaque amount was not changed. Also, depolarization of mitochondrial membrane was inhibited. As a result, pathological features of AD were decreased by CART and memory was developed in the AD model of mice *in-vivo* (Jin et al., 2015). In a similar study, when CART was pre-injected to the AD rat model, spatial memory and locomotor ability were increased. Oxidative stress that results from activation of Nrf2/HO-1 signaling was decreased by CART pre-injection and neuronal apoptosis was prevented by detecting decreasing levels of apoptotic markers. Therefore, CART may have antioxidant features in AD patients and can protect neurons against AD (Jiao et al., 2018).

CART effect on Parkinson's Disease (PD) was also investigated. Nonfunctional dopaminergic neurons and neuron terminal loss causes PD (Dauer et al., 2003). When levodopa which is used to treat PD symptoms was given to rats ip, contralateral rotations increased. Ipsilateral rotations were detected after CART injection as similar to amphetamine administration. Locomotor activities also decreased by CART by changing the activation of dopamine receptors. Therefore, CART may demonstrate protective features against PD and decreases its symptoms (Moffett et al., 2011, Upadhya et al., 2016).

The effect of CART was also investigated in other brain regions related with cognitive functions. It was the central amygdala (CeA)-ventral bed nucleus of stria terminalis (vBNST) axis which is found in the VTA. The relationship between innate fear expression, freezing response and neuron activities in this region and CART activity was assessed. Since innate fear expression and freezing response were increased by CART activity in the neurons and since NMDA receptor-mediated glutamatergic inputs were also activated by CART, it was proposed that amygdalar neurons that form and activate innate fear may be regulated by CART as well (Rale et al., 2017).

1.3. CART INDUCED SIGNALING AND BINDING STUDIES

Although CART biological actions are well studied *in-vivo* and *in-vitro*, investigations with respect to CART receptor binding are poorly understood. Several studies have been carried out to determine receptors of CART. Generally, radiolabeled ligands were used to identify receptor binding, but no specific binding was detected and receptors have thus far not been identified. However, some issues with the radiolabeling may have affected CART activity (Hunter et al., 2005). In addition, up to now binding studies are not efficient and therefore determining CART receptors has not been successful yet.

Since it is known that CART 55–102 inhibits voltage regulated Ca^{+2} influx through a G protein coupled receptor (GPCR) using the Gi/o mechanism (Figure 8) (Yermolaieva et al., 2001) and it is known that MEK and ERK downstream pathways are activated after GPCR activation, it was tested whether CART was able to activate phosphorylated-ERK (p-ERK). Therefore, p-ERK levels were examined using different cell lines like; PC12 (rat adrenal gland pheochromocytoma cell line), CATH.a (mouse catecholaminergic neuronal cell line), N2a (mouse brain neuroblastoma cell line), HEK293 (Human embriyonic kidney cell line), GH3 (rat epithelial pituitary cell line) and AtT20 cells. p- ERK levels were significantly increased only in the AtT20 and GH3 cell line. There was no increase in p-ERK for

N2a cell line (Figure 5). Therefore, CART was given to AtT20 cells in a time and dose dependent manner. Western blot results showed that p-ERK 1 and 2 were increased. The phosphorylation was inhibited by U0126 and pertussis toxin which are MEK inhibitors but not by genistein which is inhibitor for the receptor tyrosine kinase signaling (TRK) (Figure 6) (Vicentic et al., 2006). Moreover, different doses of CART 55-102 were used to check p-ERK levels in AtT20 cells. p-ERK levels were increased significantly after 10 uM, 1 uM and 100 nM CART 55-102 treatment. The inactive CART 1-27 peptide was also used, but, this did not result in an increase in p-ERK levels (Figure 7). Thus, the CART receptor may be a specific GPCR using Gi/o signaling (Figure 8) (Lakatos et al., 2005).

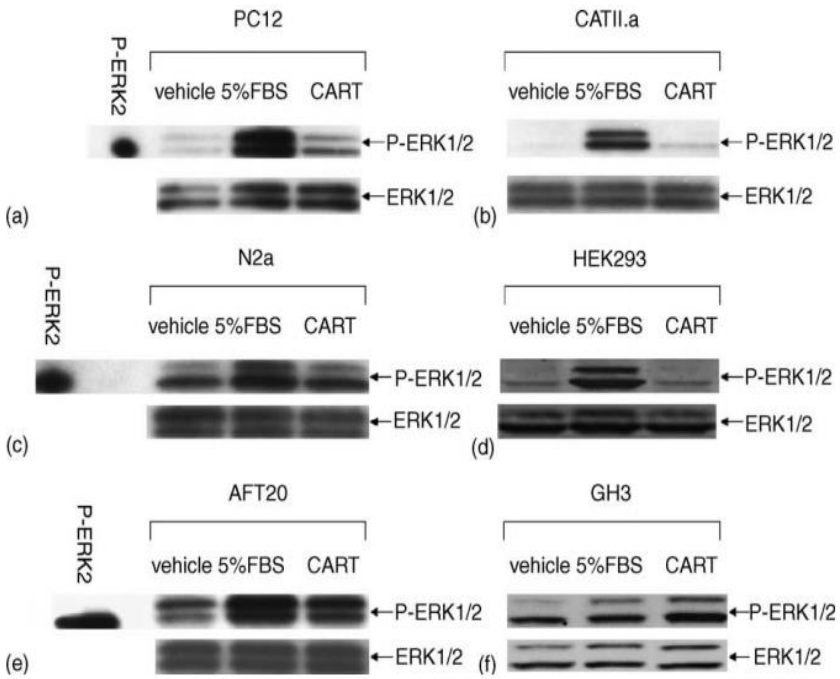

Figure 5: Activation of p-ERK in PC12, CATH.a, N2a, HEK293, GH3 and AtT20 cells. All cell lines were stimulated with either vehicle, 1 μM CART 55–102 or 5% fetal bovine serum (FBS) for 4 min. In the AtT20 and GH3 cell lines, there was a significant increase in p-ERK levels (Lakatos et al., 2005).

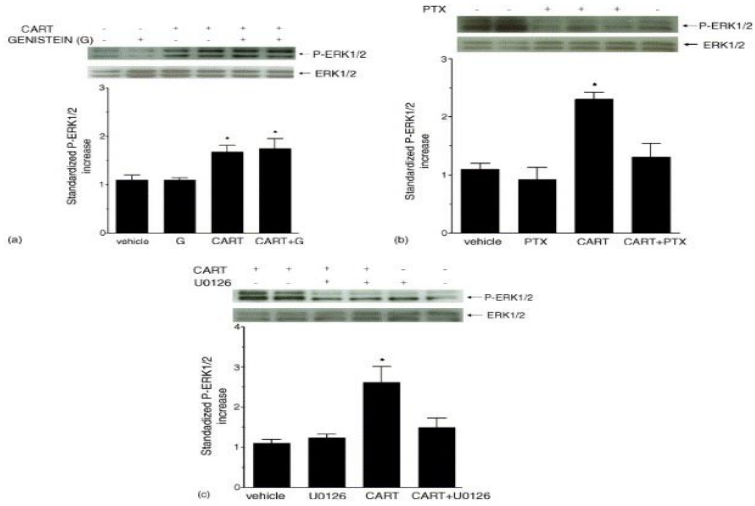

Figure 6: Effects of genistein (G) (a), pertussis toxin (PTX) (b) and U0126 (c) on CART stimulated ERK phosphorylation in AtT20 cells. After cells were treated with inhibitors, cells were stimulated with 1 μM CART for 4 min. p-ERK levels decreased after pertussis toxin and U0126 treatment, but not after genistein treatment (Lakatos et al., 2005).

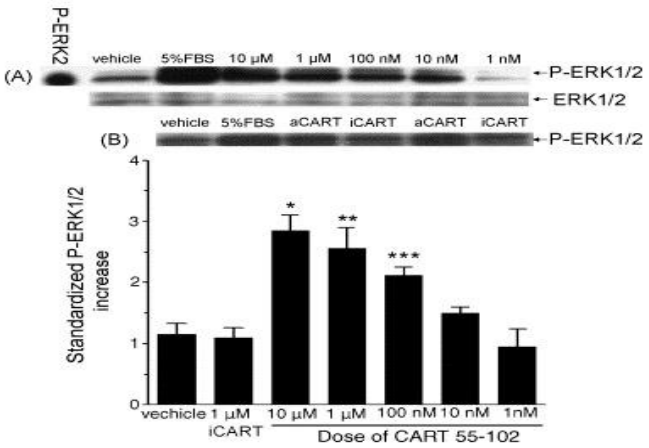

Figure 7: Dose–response curve for p- ERK1/2 in AtT20 cells. Cells were treated with varying concentrations of active CART 55–102 (aCART) and with 1 μM inactive CART 1–27 (iCART) for 4 min (Lakatos et al., 2005).

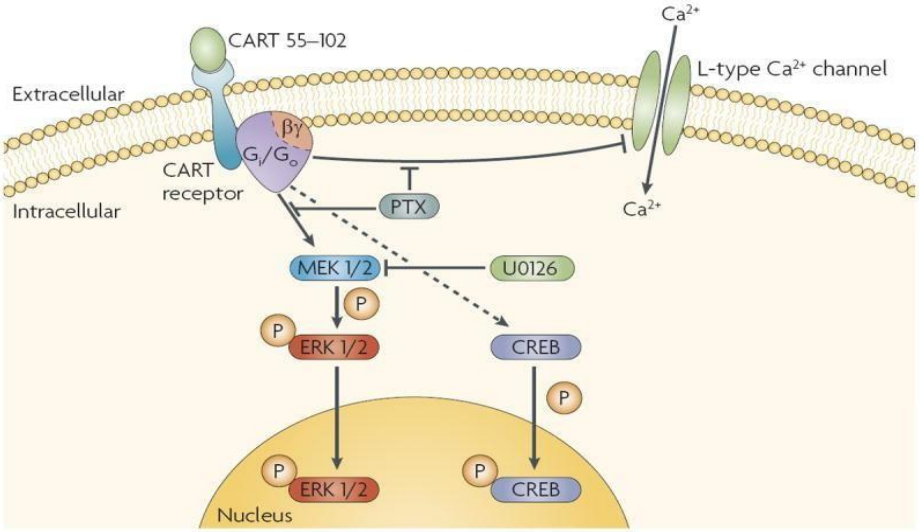

Figure 8: Proposed CART receptor signaling (Rogge et al., 2008).

In other studies, CART binding was detected in hypothalamic and HepG2 (human liver hepatocellular cells*)* cells. However, receptor binding was not detected and only CART 55–102 blocked the binding. CART 1–27 and 30–52 were also tested, but specific binding could not be detected.

After studies with CART 55-102, CART 61–102 binding studies were also performed. Radiolabeled CART 61–102 was generated, and it was only blocked with CART 55-102. There was only one site for binding. These data demonstrated that there may be a specific CART receptor in AtT20 cells (Keller et al., 2006). PC12 cells were also used in radiolabeling studies where radiolabeled CART 61–102 binding was examined. At the same time, unlabelled CART 61-102 and CART 55-102 were used as blockers. High-affinity specific binding was detected by radiolabeled CART 61–102. Moreover, as CART antagonists; PACAP 1-38 and PACAP 6-38 were used. They had low-affinity binding; however, CART binding was inhibited. These results suggested that PACAP 6-38 may be a CART receptor antagonist. p-ERK levels were also increased after CART treatment and PC12 cell differentiation. p-ERK activation was prevented by pertussis toxin and PACAP 6-38.

This again showed that CART binding managed through GPCR (Lin et al., 2011).

Besides binding studies, the effect of CART 55-102 on Ca^{+2} signaling was assessed on cocaine stimulated Ca^{+2} influx into the rat neurons showing that voltage regulated Ca^{+2} signaling was prevented by CART 55-102. CART 55-102 exerted its effect by inhibiting the L-type voltage-gated Ca^{+2} channel activity. Activity was changed by regulating a G-protein-dependent pathway. These results suggested that CART 55-102 acts like a homeostatic feedback response and exerts its effect by using a GPCR (Yermolaieva et al., 2001).

Structural studies of CART showed that CART 55-102 and CART 61-102 have three disulfide bridges and a similar biological activity. To understand the effect of these disulfide bridges on activity, natural CART 61-102 which has three disulfide bridges and its analog CART 61-102 which has one or two disulfide bridges were examined and compared. Analog CART 61-102 was prepared by changing the aa at position 67 with another aa to make the one disulfide bridge which positioned between the 68-86 aa interval useless. This analog was found to bind PC12 cells with high affinity and icv administration of this analog to mice showed anorectic effects on mice. Therefore, the study demonstrated that disulfide bridges between cysteines 68 and 86 were not required for activity of CART 61–102 but the other two bridges were required for the peptide activity and perhaps for a specific structure for receptor activity (Blechova et al., 2013).

Furthermore, there may be multiple CART receptors. Since CART 55–102 and CART 62– 102 peptides are known to have many functions in the areas of feeding, metabolism, energy expenditure, stress, reward, drug tolerance, it is thought that CART peptides may induce many signal pathways in the cells (Sarkar et al., 2004). Synthetic CART fragments which are produced from CART precursor had also biological activity in mice neurons. Hyperlocomotion that results from morphine addiction was decreased by these fragments as seen in the CART 55-102. Therefore, there may be many CART receptors for different types of CART fragments and

natural CART peptides (CART 55-102 and CART 62-102) (Dylag et al., 2006).

To identify receptors of CART, receptor clones can be formed in N2a cells for future studies. N2a cells can be used for cloning because it was shown that N2a cells are not be able to increase p-ERK levels by CART treatment (Figure 5) (Lakatos et al.,2005). Identification of CART receptors may lead to discovery of functions related to CART and receptors may be a target for pharmacological studies (Vicentic et al., 2006).

1.4. HYPOTHESIS AND AIM

1.4.1. HYPOTHESIS

Considering that a Gi/Go coupled GPCR is involved in CART signaling, microarray data that measured the mRNA levels of a comprehensive profile of non-chemosensory GPCRs were analyzed by our group (Merve Kasap, M.Sc. Master thesis, 2014, METU Biological Sciences, Ankara). Expression levels of 7 selected GPCR genes (*SCTR, GRM1, GLP1R, GLP2R, CASR, GLP133* and *GLP116)* were verified in the AtT20 cell line and these genes were determined as candidate CART receptor genes which are members of different subfamilies of GPCRs. In this study, it was hypothesized that CART associated that were previously determined candidate genes by our group could increase p-ERK 1/2 and might be potential candidate CART receptors.

1.4.2. AIM

Seven different candidate CART receptor genes detected by bioinformatic approaches by our group were transfected to N2a cells as a CART nonresponsive cell line. Then N2a cells were stimulated with CART 62-102 peptide to activate the signal transduction pathway for a GPCR. Finally, p-ERK 1/2 response was analyzed using anti-p-ERK 1/2 staining and western blot. Increasing levels of p-ERK 1/2 by the transfected candidate CART receptor genes could be used to identify potential genes of interest that could serve as the unknown CART receptors.

CHAPTER 2

MATERIALS AND METHODS

2.1. Verification of Candidate CART Receptor Genes in Plasmids

Using microarray studies, over a thousand GPCR signaling related gene products were analyzed in order to detect candidate CART receptor genes. Seven candidate genes were determined to be possible CART peptide receptors (Merve Kasap, M.Sc, Master thesis, 2014, METU Biological Sciences, Ankara). The plasmids purchased from ADDGENE (Massachusetts, USA) were *SCTR, GRM1, GLP1R, GLP2R, CASR, GLP133* and *GLP116* and all of them are known to be GPCRs (Kroeze et al, 2015). These candidate genes were expressed in TANGO vectors of which the original backbone is pcDNA3.1 (+). The vectors were isolated from bacterial cells (E.coli, DH5α strain) and bacteria in agar stabs were kept in 4°C fridge for two weeks. For longer storage, bacteria were in – 80°C as glycerol stocks.

2.1.1. Streak Plates of Bacterial Cells and Colony Selection

Bacteria (DH5α competent E. coli) were inoculated onto the LB agar plates containing Ampicillin (1000 u/mL). For each of the seven different plasmids, agar plates were prepared.

For 14 agar plates; 5 gr NaCl, 5 gr tryptone and 2.5 gr yeast extract was put in a glass bottle and dH_2O was added until it reached 500 mL.

Mixture was swirled using a magnetic stirrer. After swirling, the stirrer was taken out and the bottle was placed into the autoclave (Nuve Sanayi, Ankara, Turkey) for 20 minutes at 121°C. After autoclaving, the agar solution was allowed to cool down to 55°C. For 500 mL liquid agar solution, 500 µl 1000 u/mL Penicillin/ Streptomycine antibiotic solution was added to the bottle and the solution was

poured onto the agar plates sterily. Lids were placed on the plates and plates were allowed to cool for 60 minutes until they were solidified and inverted. The plates were labeled with antibiotic concentration and stored in plastic bags at 4°C. Before usage, plates were kept at 37°C for half an hour and after that, bacteria were inoculated onto the plates by using the streak plate method and they were incubated at 37°C in the incubator (5% CO_2) overnight.

DH5α competent cells were inoculated on 7 different plates and then, grown on the agar plate. From each plate, one separate colony was selected and inoculated into fresh LB agar plates to obtain clonal bacterial cells.

LB liquid media was prepared by using the LB broth powder of which 2.5 gr powder was added to 100 mL liquid media and autoclaved. Liquid medium was used for plasmid isolation and one specific colony was placed in 15 mL falcon tubes that contain 3 mL LB liquid media. The tubes were incubated at 37°C overnight in a ZHWY-200b incubator with shaker (Zhicheng, Shanghai, China).

2.1.2. Plasmid Isolation

After cells were grown in the media, plasmid isolation was carried out using the GeneJET Plasmid Miniprep Kit (Thermo Fisher Scientific, Rockford, USA). Briefly, the bacterial culture was centrifuged at 8.000 rpm for 2 minutes at room temperature. Supernatant was removed and the pellet was resuspended by using 250 µl of resuspension solution. Then, 250 µl lysis solution was added and eppendorf tubes were inverted 4-6 times. Likewise, 350 µl neutralization solution was added and again tubes were inverted 4-6 times and centrifuged for 5 minutes. Afterwards, supernatant was transferred to GeneJet Spin Columns and columns were centrifuged for 1 minute. To wash the column, 500 µl of washing solution was added to the columns and columns were centrifuged for 1 minute. Flow through was discarded. This washing process was repeated for 2 times. After that, an extra centrifugation was carried out for 1 minute. Finally, to elute the purified DNA, columns were transferred into new eppendorf tubes and 50 µl of elution buffer was added to each

column and incubated for 2 minutes. Next, the tubes were centrifuged for 2 minutes at 13.000 rpm two times and purified plasmid DNA was collected.

After isolation, to test DNA purity, Nanodrop (BioDrop, Cambridge, UK) was used. For pure DNA, A260/280 ratio must be between the ranges of 1.8 and 2.00 and A 260/230 must be between the ranges of 2.00 and 2.20 (William et al., 1997) (Appendix A, Table A.1).

2.1.3. Restriction Digestion of Candidate CART Receptor Genes by NotI Enzyme

The candidate CART receptor genes were digested with NotI restriction enzyme to make the plasmid DNA linear and to verify presence of gene. To test one of them, the GPR116 plasmid was digested by NotI using 0.3 µg of plasmid. NotI enzyme (Thermo Fisher Scientific, Rockford, USA) was used at 10 U/ µl. This enzyme was supplied with 1 mL of 10X Buffer O and 1 mL of 10X Buffer Tango. The buffer O was the best buffer for the NotI enzyme activity (100%). The protocol was performed according to the manufacturer`s instructions and 16 µl nuclease free water, 2 µl 10 X Buffer O, 0.3 µg of plasmid DNA and 2 µl NotI enzyme were added to an eppendorf tube, gently mixed and incubated at 37°C for overnight.

2.1.4. Agarose Gel Electrophoresis

To prepare a 1% agarose gel, 0.5 gr agarose powder was mixed with 50 mL 1X TAE buffer in a beaker and placed in the microwave till the agar was dissolved. Then, 1 µl ETBr was added and shaken slowly. After cooling shortly in room temperature, it was poured in a container and allowed to solidify for 30 minutes. After solidification of the gel, 1X TAE buffer was poured onto the container until the buffer covered the gel completely. DNA samples were prepared with a 6X loading dye and 1 µl dye and 5 µl sample were mixed and loaded onto the gel. The gels were run at 100 V for 90 minutes. Lastly, the gel was imaged with UV light by using Imaging and Analysis Instrument (Appendix G, Figure G.1). As reference sequences (Ladders); O'GeneRuler 1 kb Plus DNA Ladder (Thermo Fisher

Scientific, Massachusetts, USA) and DirectLoad 50 bp DNA Step Ladder (Sigma Aldrich, Missouri, USA) were used (Appendix B, Figure B.1 and B.2). Sizes of these ladders are shown in Appendix B.

Five µl of the remaining, undigested other 5 plasmids were also loaded onto the 1% agarose gel (GPR133, GLP2R, GLP1R, GRM1, CASR plasmid DNAs) by using the 2 sets of agar plates (Appendix G, Figure G.2). Plasmid isolation of all genes was carried out as summarized above. Nanodrop (BioDrop, Cambridge, UK) was used to measure DNA concentration and purity (Appendix A, Table A.2, A.3).

2.1.5. Primer Design for SCTR

Primers were designed using the ADDGENE website, NCBI Gene, Uniprot KB databases and rules of IDT Oligo designer (Appendix B, Table B.3).

2.1.6. PCR for SCTR Genes

PCR was carried out by using the old SCTR plasmid DNA. First, a gradient PCR was carried out to find out the optimal annealing temperature (Darren et al, 2008). Gradient PCR was performed for the primers with temperatures ranging from 57 to 68°C. Nine tubes were inserted at 9 different temperatures and other thermal cycler temperature adjustments were carried out according to the steps indicated in Appendix B, Table B2 using a Bio-Rad thermal cycler (Singapore City, Singapore). The amplified DNAs were loaded onto the 1% agarose gel and imaged (Appendix G, Figure G.3).

After the PCR protocol was optimized (Appendix B, Table B.1), it was run with an initial denaturation step at 94°C for 2 minutes to activate Taq polymerase and denature DNA fragments. Thus DNA fragments will change its structure from double stranded to single stranded so primers could bind to the specific sites of the gene. Another round of denaturation at 94°C was performed for 30 seconds. Annealing temperatures for SCTR was used at 64°C for 30 seconds. This specific temperature allows the primers to bind to the specific regions of the DNA. An

extension procedure which allowed Taq polymerase to amplify the selected gene of interest was set up at 74°C for 2 minutes. Denaturation, annealing and extension procedures were then repeated for 40 cycles and ended with final extension at 74°C for 5 minutes and incubation at 4°C indefinitely.

2.1.7. Agarose Gel Electrophoresis of SCTR Genes

SCTR genes were amplified at 64°C for PCR and PCR products were analyzed in 1% agarose gel (Appendix G, Figure G.4). Then, 5 µl of undigested SCTR plasmid DNA, digested SCTR plasmid DNA, PCR product of digested *SCTR* were loaded with DNA ladder to the 1% agarose gel (Appendix G, Figure G.5).

2.1.8. Colony Selection

To detect full plasmid size for all genes, three different, separate colonies for each gene were selected from the plates. After that, plasmid isolation was carried out for each colony using the same protocol and Nanodrop was used to measure purity and concentration of the samples (Appendix A, Table A.1, A2, A3).

For imaging, all plasmid DNAs were digested with 0.5 µl of NotI enzyme and DNA concentrations were adjusted to 0.5 µg/µl for each plasmid. Two µl Buffer O and 16 µl nuclease free water were used for the digestion reactions. All reaction tubes were kept in 37°C incubator for 16 hours. After digestion, plasmid DNAs were loaded onto 2% agarose gel (Appendix G, Figure G.6, G.7, G. 8). Before loading, DNA samples were mixed with loading dye; for each sample; 5 µl plasmid DNA + 1 µl DNA loading dye (6X) were prepared.

2.1.9. Next Generation Sequencing of SCTR

Plasmid DNA was sent to Sentegen (Bilkent University, Ankara) for New Generation Sequencing (NGS) to sequence one of the SCTR genes (Appendix G, Figure G.11).

2.1.10. Primer Design for TANGO Vector

Two primers were selected from the TANGO vector by using the ADDGENE gene analyzer. These primers cover the sites of near the gene insertion. They were bought from İONTEK (İstanbul, Turkey) (Appendix B, Table B.4).

2.1.11. PCR for 7 Candidate Genes with TANGO Primers

PCR was carried out for all genes with general TANGO primers using the PCR protocol in Appendix B, Table B.1 and PCR products of all genes were run on a 1% agarose gel (Figure 9).

2.1.12. Sequencing and Analysis of GLP1R and GLP2R Genes

Plasmid DNAs were sequenced for *GLP1R* and *GLP2R* (Appendix G, Figure G.13, G.14) by DNA sequencing services (BM Laboratuvar Sistemleri, Ankara) that applied Sanger Sequencing. Universal T7 forward primer and BGH reverse primer were used for sequencing and two forward primers were also designed for both *GLP1R* (Appendix G, Table G.1) and *GLP2R* (Appendix G, Table G.2) to allow Sanger sequencing to read the sequences from the beginning part of the open reading frame (ORF) to the final part of the ORF. Sequences were exported into "Basic Local Alignment Search Tool" (BLAST, especially Blastn) available from the website of National Center for Biotechnology Information (NCBI-http://www.ncbi.nlm.nih.gov) to identify matches with existing characterized reference sequences (NCBI Gene ID for *GLP1R*: 2740 and Gene ID for *GLP2R*: 9340).

2.2. Cell Culture Studies

The human embryonic kidney cell line (HEK293, kind gift of Jack A. Yanovski, MD, PhD, Section on Growth and Obesity, NIH, USA) and mouse neuroblastoma cell line N2a (ATCC, Virginia, USA) were grown on T25 and then in T75 cell culture flasks (Thermo Fischer Scientific, Massachusetts, USA).

2.2.1. Cell Passaging

Frozen cells were collected from the liquid nitrogen phase and T25 flasks were prepared with 3 mL of complete medium (CM) (Appendix C) after which it was placed into the 37°C incubator at 5% CO_2 (Heracell 150i, Thermo Fisher Scientific,Massachusetts, USA).. Cells were thawed in a 37°C water bath for 2 minutes until the vial contents were thawed completely. Then, the vial was decontaminated with 70% ethanol and opened under strict sterile conditions under the laminar flow cabinet. Vial contents were resuspended in 9 mL CM and centrifuged at 1500 rpm for 7 minutes. The cell pellet was resuspended in 1 mL of CM and the suspension solution was added to the T25 flask containing 3 mL CM. The flask was gently mixed and placed into the incubator. Cells were grown to a confluency of 70-80% and controlled every day for their viability. Generally, 4-5 days later, cells demonstrated their specific cell shapes under the microscope. When cells reached 70% confluency, they were split into a new T75 flask.

2.2.2. Total Protein Isolation of HEK Cells and N2a Cells

To isolate proteins, M-PER (Mammalian Protein Extraction Reagent, (Thermo Fisher Scientific, Rockford, USA) was used with added protease inhibitors such as complete mini EDTA-free protease inhibitor cocktail tablets (working concentration; 7X in 1.5 mL distilled water, Roche, Basel, Switzerland) and phophatase inhibitor-Mix II solution (1 mL for 100 mL tissue extract, SERVA Electrophoresis GmbH, Heidelberg, Germany).

To isolate total proteins from HEK293 cells, first, the culture medium was removed from the T75 flask and cells were washed once with 3 mL PBS to not interfere with the subsequent protein analysis and to remove phenol red from the cells. To extract proteins; 400 µl M-PER, 37.5 µl protease inhibitor and 8 µl phosphatase inhibitor was prepared and added to T75 flasks and they were shaken for 2-3 minutes gently. The lysate was collected to the eppendorf tube and centrifuged at 14.000 rpm for 7 minutes to pellet the cell debris.

Supernatant was collected into a new eppendorf tube for analysis. Likewise, for 6 wells, 250 µl M-PER, 20 µl protease inhibitor and 5 µl phosphatase inhibitor were mixed and collected samples were stored at -20°C.

2.2.3. Bradford Assay Protocol

Protein concentrations were measured with the Coomassie Plus (Bradford) Assay Kit (Thermo Fisher Scientific, Rockford, USA). First, a standard curve was generated by using different known concentrations of Bovine Serum Albumin (BSA) (SERVA Electrophoresis GmbH, Heidelberg, Germany). The BSA stock solution in 2 mg/mL was diluted as in Table 1.

Table 1: Preparation of Diluted Albumin (BSA) Standards.

Dilution Scheme for Standard Test Tube and Microplate Protocols (Working Range = 125–1500µg/mL)

Vial	Volume of Diluent	Volume and Source of BSA	Final BSA Concentration
A	0	300µL of Stock	2000µg/mL
B	125µL	375µL of Stock	1500µg/mL
C	325µL	325µL of Stock	1000µg/mL
D	175µL	175µL of vial B dilution	750µg/mL
E	325µL	325µL of vial C dilution	500µg/mL
F	325µL	325µL of vial E dilution	250µg/mL
G	325µL	325µL of vial F dilution	125µg/mL
H	400µL	100µL of vial G dilution	25µg/mL
I	400µL	0	0µg/mL = Blank

Seven ul of these standards and unknown protein samples were pipetted in a 96 wells plate (Corning, NY, USA). Then 250 µl of Coomassie Plus Reagent was added onto the protein samples. For each diluted BSA and unknown protein samples, samples were pipetted in triplicate. The plate was placed in spectrophotometer (Thermo Fisher Scientific, Vaatan, Finland). The plate was shaken for 30 seconds then incubated at room temperature for 10 minutes in the machine. Absorbance was measured at a wavelength of 595 nm and results were recorded in an excel file.

To calculate the standard curve graphic, the average of the 595 nm measurement for the blank replicates was subtracted from 595 nm measurements of all standards

and unknown samples. The standard curve was plotted by using the subtracted values to calculate protein concentration in µg/mL. Results of protein concentrations were shown in Appendix D, Table D1, D2, D3.

2.2.4. Primary Antibody Verification with Dot Blot

Dot blot method was used to control the quality of the primary antibody p-ERK1/ERK2 (Tyr204) polyclonal antibody (Catalog number: PA5-36776, Thermo Fisher Scientific, Rockford, USA) and its working concentration by using the HEK293 cells proteins. For the dot blot protocol, TBS, TBS-T and BSA/TBS-T were prepared as indicated in the Appendix E.

Four pieces of nitrocellulose membrane were used for the dot blot experiment. Circles were drawn onto each membrane by a pencil and then 2 µl of protein samples were spotted in the middle of the circles. Membranes were allowed to dry 15 or 20 minutes. Then non-specific sites were blocked with 5% BSA/TBS-T for one hour at room temperature. Next, membranes were incubated with primary antibody (p-ERK1/2) (1/1000 diluted) diluted in 3% BSA/TBS-T for 30 minutes at different concentrations (Appendix E, Table E.16). Then membranes were washed with TBS/T for 3 times, each 5 minutes and incubated with secondary antibody (1/5.000) (anti-rabbit IgG antibody, Cell Signalling Technology, Massachusetts, USA) diluted in 3% BSA/TBS-T for 30 minutes. Membranes were washed with TBS-T for 3 times (15'- 1.5'- 2 minutes) and TBS for 5 minutes. Finally, membranes were incubated with ECL reagent (BioRad, California, USA) for 1 minute, covered with Saran wrap and exposed to UV light by using the BioRad imaging system (BioRad, California, USA).

2.2.5. Transfection of N2a Cells with TANGO Vectors

To express the genes of interests in N2a, the transfection protocol was carried out using Lipofactemine2000 protocol according to the manufacturer`s instructions. First, N2a cells were detached to transfer cells to a 6 wells plate from T75 flasks. To detach cells from the T75 flasks, old medium was removed and 3 mL Trypsin/EDTA

solution (0.05% Trypsin/ 0.02 EDTA in DPBS) was added to the flask and placed in 37°C incubator until the cell layer was detached. Then, 7 mL CM was added to the flask to decrease Trypsin/EDTA effects on cells and they were suspended in the flask. The cell suspension was placed into fresh wells. Approximately $0.3x10^6$ cells were seeded to obtain a cell number of $1.2x10^6$ after one day. Next day, cells were transfected with 2 µg plasmids in separate eppendorf tubes containing 2.5 µl lipofectamine reagent and 100 µl opti-MEM solution and incubated at room temperature for 20 minutes. In another tube, 2 µg DNA and 100 µl opti-MEM solution was mixed and incubated for 20 minutes. Just before 20 minutes incubation, CM was removed from cells and they were washed with 1 mL PBS prewarmed at 37°C. Then, the two solutions were mixed and added to the cells drop by drop. The cells were incubated for 3 hours in the incubator and 3 hours later, an additional 1 mL CM was added onto the cells. The next day, the medium was removed and 2 mL new fresh CM was added onto the cells and they were incubated for another day.

2.2.6. CART Stimulation of Transfected N2a Cells

N2a cells were stimulated with 10 µM CART 62-102 (code: EK-PC-003-61, Phoenix Pharmaceuticals, California, USA). Before protein isolation, transfected N2a cells were stimulated with 10 µM CART 62-102 peptide for 5 and 10 minutes, as indicated in Lakatos et al (2005).

2.3. Western Blot Assay

The Western Blot assay can be divided into two stages; SDS PAGE gel electrophoresis and transferring the gel proteins from the gel to a polyvinylidene fluoride (PVDF) membrane which will be required for primary and secondary antibody binding. The Western blot protocol was listed in Appendix F and protocol was adapted from Lakatos et al, 2005. Separating and stacking gels and all buffers that were used for all steps are listed in Appendix E.

Mouse anti-rabbit IgG HRP secondary antibody was from Santa Cruz Biotechnology (Dallas, Texas, USA). For the reference size; PageRuler Plus

Prestained Protein Ladder 10 to 250 kDa (Thermo Fisher Scientific, Massachusetts, USA) was used for all Western blot experiments. Reference size for protein was depicted in Appendix F, Figure F.1.

CHAPTER 3

RESULTS

3.1. Verification of 7 Candidate CART Receptor Genes In TANGO Vectors

Nanodrop measurements of old candidate CART receptor plasmid DNAs from our research team (Merve Kasap, M.Sc thesis, 2014, METU Biological Sciences, Ankara) were not between the range of 1.8- 2.0 for A260/280 ratios. Only A260/280 ratios of *GPR116* and *SCTR* were 1.8, therefore, the size of these two genes; GPR116 gene and SCTR gene was determined and plasmid DNAs of *GPR116* and *SCTR* were restricted with NotI enzyme to make the DNAs linear. The size of the TANGO vectors for *GPR116* and *SCTR* should be 6632 bp and as depicted in Appendix G, Figure G.1, the size of the TANGO vectors for *GPR116* and *SCTR* was actually in that range. For the other 5 plasmid DNAs, there were no bands on the agarose gels (not shown). Therefore, all candidate genes were newly purchased from ADDGENE (USA) and called new CART receptor candidate genes.

Among the purchased 7 new genes, GPR133, GLP2R, GLP1R, GRM1, CASR plasmids DNAs were digested with NotI enzyme and loaded to the 1% agarose gel. Also, old plasmids of these five genes were loaded onto the same agarose gel to detect any difference between them (Appendix G, Figure G.2). Two bands were detected for each gene. After restriction digestion reaction, if nicked, supercoiled and linear DNAs were detected on same agarose gel, this means that restriction digestion reaction was not carried out properly and the vectors were uncut. Therefore, restriction digestion reaction was repeated for many times but in our results, there were always nicked, supercoiled and linear DNAs for these 5 genes.

The band for the SCTR plasmid DNA was detected in agarose gel correctly (Appendix G, Figure G.1), to amplify our specific gene site by PCR, primers were

designed for *SCTR* as in Appendix B, Table B.3. The PCR protocol was carried out for only *SCTR* to test one of the genes. Since optimum annealing temperature was not known, first, a gradient PCR was performed and tested at 9 different temperatures. Amplification of the target gene was detected at an annealing temperature of 64°C (Appendix G, Figure G.3). These primers were also used for new SCTR genes to check presence of the genes in the new plasmids (Appendix G, Figure G.4). The figure showed that there was no gene amplification for the new plasmids. The size of old SCTR genes was accurate and therefore used as a positive control. Since, the presence of SCTR was not detected (Appendix G, Figure G.4), new SCTR plasmid DNAs; undigested, digested *SCTR* and its PCR products were tested on the agarose gel (Appendix G, Figure G.5). Band sizes of the undigested and digested *SCTR* were almost 6632bp which was accurate for TANGO vector. However, there was no band again for the PCR product of digested *SCTR* which must be seen as 1320 bp.

Due to not detecting a band for the PCR product of *SCTR*, bacterial cells were again inoculated. Nanodrop results of isolated plasmids were recorded in Appendix A, Table A1, A2, A3. They were loaded to the 2% agarose gels in three parts. Part 1 (Appendix G, Figure G.6) shows *CASR, SCTR* and *GPR116*. Part 2 (Appendix G, Figure G.7) shows *GLP2R, GLP1R* and *GRM1*. Part 3 (Appendix G, Figure G.8) shows old *SCTR, GPR133* and *CRHR1*. As a result, the new *SCTR* size was appropriate for TANGO vector (6632 bp) and they were accurate (Appendix G, Figure G.6), therefore PCR was performed for those. However, there was no SCTR gene amplification for the new plasmids either, but, there was SCTR gene amplification for the old SCTR genes as a positive control (Appendix G, Figure G.9). Hence, a sample of SCTR plasmid DNA was sequenced by the next generation sequencing in Sentegen (Bilkent University, Ankara) to determine the real base number of the plasmid DNA and existence of the gene in the TANGO vectors (Appendix G, Figure G.10 and G.11). As sequencing data indicated, the SCTR sequence (1320 bp) could not be detected in the TANGO vector (Appendix G,

Figure G.11). Therefore, all experiments and analyses proved the absence of *SCTR* in the TANGO vector.

3.2. Selection of New Primers for the TANGO Vector

New plasmid DNAs were chosen from the website of ADDGENE. These primers were T7 forward primer and BGH reverse primers for the general TANGO vector (Appendix B, Table B.4)

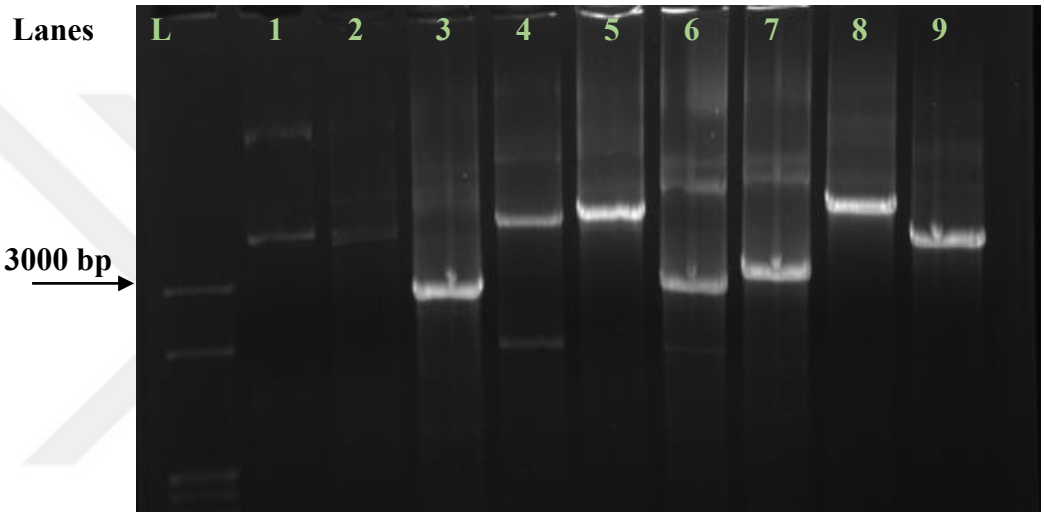

Figure 9: Agarose Gel Image of PCR for the 7 Candidate CART Receptor Genes. Lane 1: New SCTR, Lane 2: CRHR1, Lane 3: New SCTR, Lane 4: CASR, Lane 5: GRM1, Lane 6: GLP1R, Lane 7: GLP2R, Lane 8: GPR116, Lane 9: GPR133. Ladder (L): DirectLoad™ 50 bp DNA Step Ladder. (All genes were new plasmid DNAs).

In Figure 9, the size of the genes must be the following, *CRHR1*: 1332 bp, *CASR:* 3264 bp, *GRM1:* 3582 bp, *GLP1R:* 1389 bp, *GLP2R*: 1659 bp, *GPR116*: 4038 bp, *GPR133*: 2622 bp, *SCTR*: 1320 bp. However, the size of the genes was detected more than their actual insert size because of additional sequences came from PCR (additional TetR gene) (Appendix G, Figure G.12). Sanger sequencing

results of *GLP1R* and *GLP2R* (Appendix G, Figure G.13, G.14) showed that these two genes are present in the TANGO vectors. Additional sequences came from the TetR gene that is found in the open reading frame. Therefore, the size of *GLP1R* and *GLP2R* was correct (Figure 9). Remaining 5 genes sequencing were not performed but band sizes of those plasmid DNAs were also more than their actual sizes which may be because of the TetR gene. Therefore, Figure 9 showed that there were *GLP1R* and *GLP2R* in the TANGO vectors and band sizes of other 5 genes were also expected. For the new SCTR gene, two different tubes of plasmids were used and there was SCTR gene in only one selected colony (Lane 3 in Figure 9).

The flow of the rest of the experiments was the transfection of N2a cells with TANGO vectors. Then, cells were stimulated with 10 µM CART 62-102 for 10 min and 5 min and proteins were collected for each gene to be analyzed for the existence of p-ERK 1/2.

3.3. Dot Blot Analysis

The dot blot protocol was carried out by using HEK293 proteins to verify primary antibody quality and working concentration. HEK293 protein concentrations were calculated by the Bradford assay.

p-ERK 1/2 primary antibody was diluted in 3% BSA-0.05 (v/v) T-TBS (10 mL) for different concentrations (Appendix E, Table E.16). Nitrocellulose membrane was used and for each dilution, 3 dots were dispersed on the membrane to work as triplicate (Figure 10).

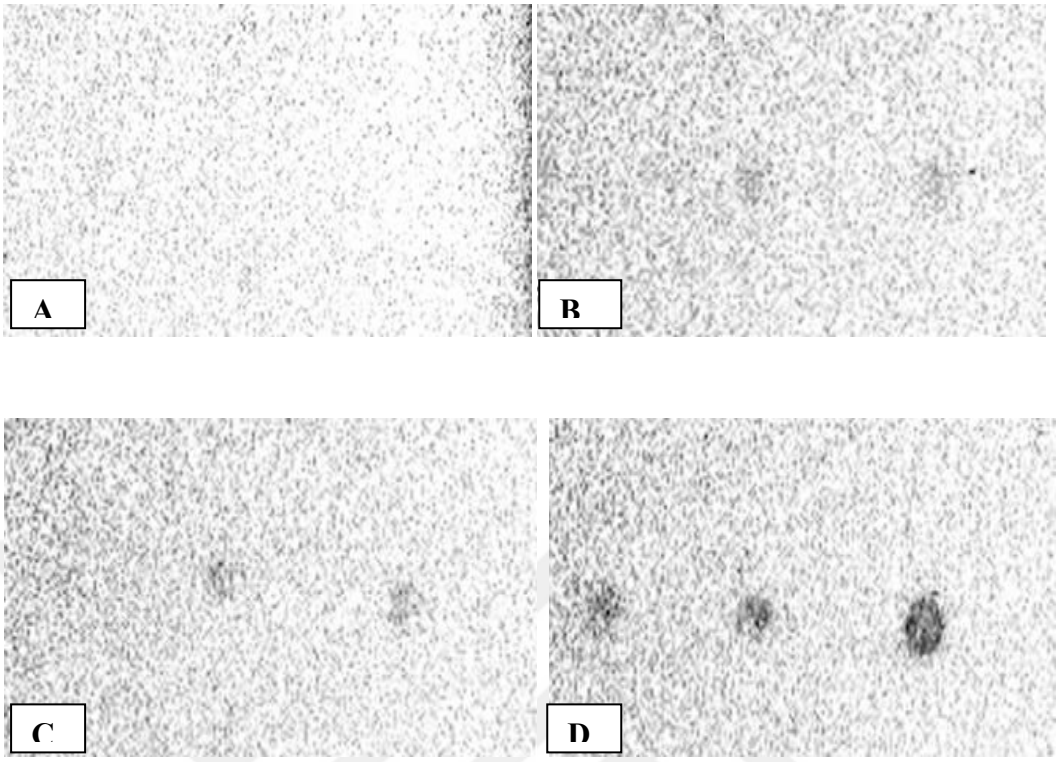

Figure 10: Dot Blot Imaging. A) 1/10000 diluted anti-p-ERK1/2 and **B)** 1/5000 diluted anti-p-ERK1/2, **C)** 1/2000 diluted anti-p-ERK 1/ 2 and **D)** 1/1000 diluted anti-p-ERK1 /2.

The 1/1000 dilution of p-ERK 1/2 showed best results on the nitrocellulose membrane (Figure 10), therefore, this dilution was used for anti-p-ERK1/2 in further Western blot experiments.

3.4. Western Blot Analysis

After loading an equal amount of proteins (50 µg) for 7 candidate receptor genes on SDS-PAGE gels, they were analyzed using with anti-p-ERK 1/2 by Western blot (Figure 11, 12).

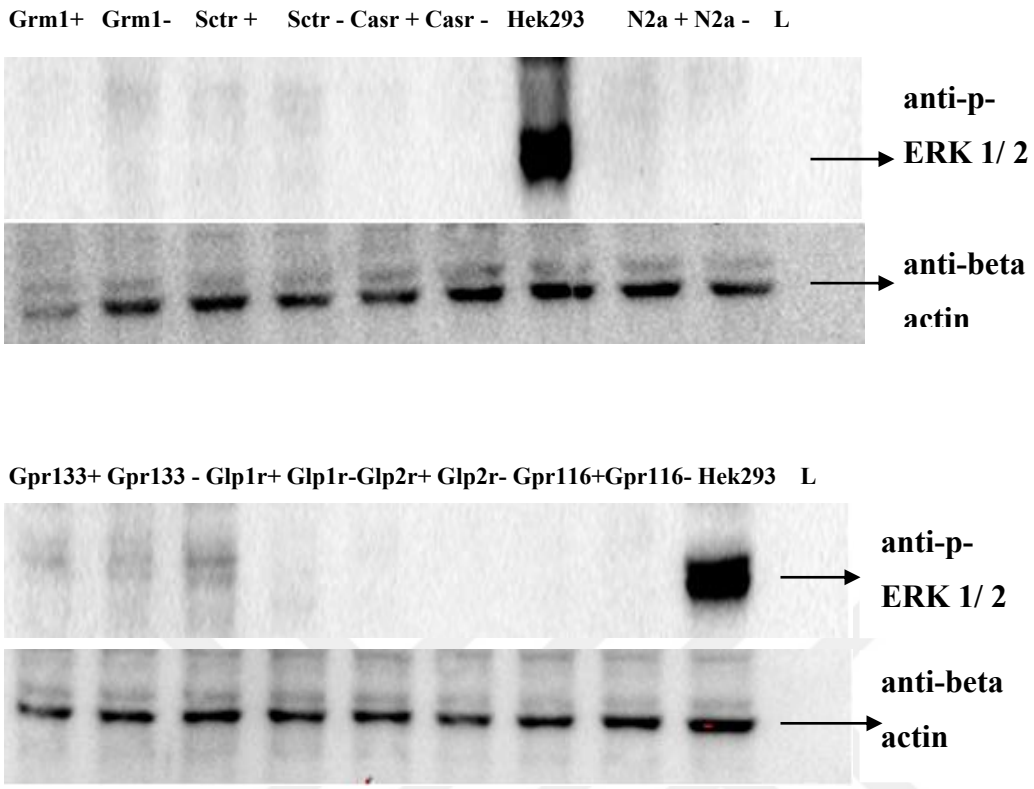

Figure 11: Western Blot Image of 5 minutes CART stimulated N2a. Ten µM CART stimulated N2a cells probed with anti-p-ERK 1/2 and anti-beta actin**.** All proteins (50 µg) for 7 genes (*SCTR, GLP1R, GLP2R, GRM1, CASR, GPR116, GPR133*) were loaded onto the gel. The cells were stimulated for 5 minutes with CART 62-102. (+: transfected cells were stimulated with CART, - : transfected cells were not treated with CART) (Number of transfections: 5).

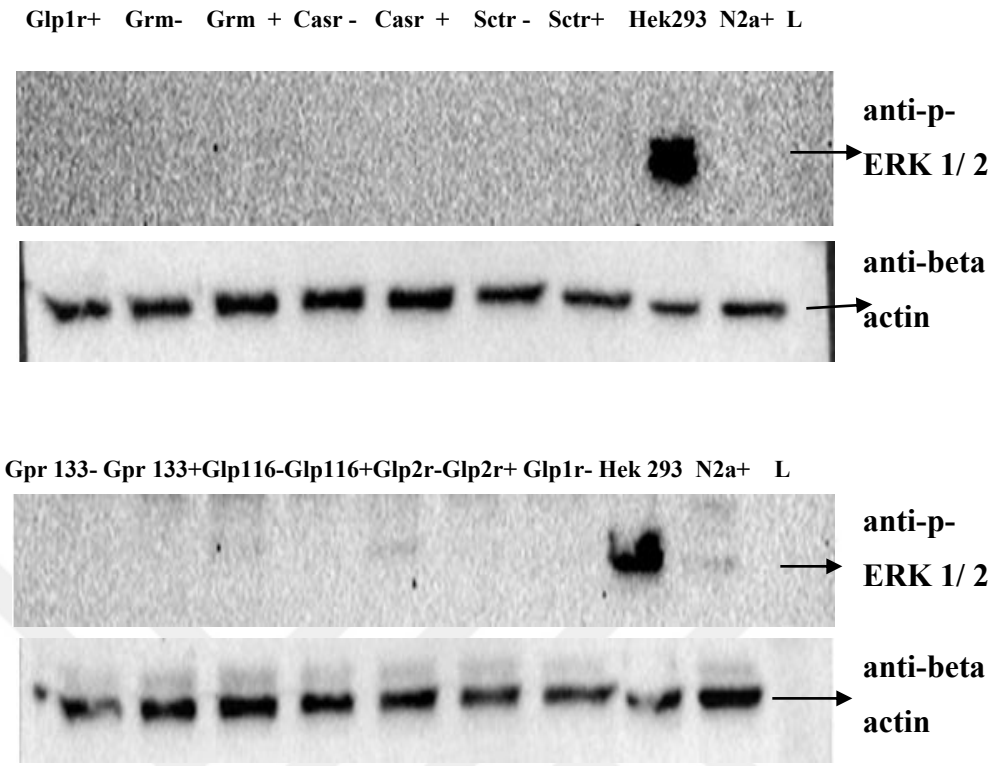

Figure 12: Western Blot Image of 10 minutes CART stimulated N2a. Ten µM CART stimulated N2a cells probed with anti-p-ERK 1/2 and anti-beta actin. All proteins (50 µg) for 7 genes (*SCTR, GLP1R, GLP2R, GRM1, CASR, GPR116, GPR133*) were loaded onto the gel. The cells were stimulated for 10 minutes with CART 62-102. Rightmost part of the image is the protein ladder where the sizes of the fragments are listed. (+: transfected cells were stimulated with CART, - : transfected cells were not treated with CART) (Number of transfections: 4).

p-ERK 1/2 band (42-44 kDa) was only detected in the positive control HEK293 cells and there was a slight increase in GLP1R gene transfected cells that were treated with CART for 5 minutes (Figure 11). Other 6 genes transfections did not result in a signal for p-ERK 1/2. Beta-actin bands (42 kDa) showed that the loading of proteins was accurate (Figure 11 and 12).

CHAPTER 4

DISCUSSION

Previous studies related to CART functions have demonstrated that there are many effects of CART on the body. CART peptides are strongly associated with a role in feeding, satiety, obesity, type 2 diabetes and energy metabolism. Moreover, they are expressed during reward mechanisms in specific brain regions. Drug behavior, psychostimulants, stress, anxiety, cognitive functions are all affected by CART peptides (Douglas et al., 1995; Tim et al., 1999; Vicentic et al., 2007). CART peptides are also produced in the peripheral nervous system. There, it functions on the gastrointestinal system, cardiovascular system, kidney and liver (Abels et al., 2016; Romeu et al., 2018; Matsumura et al., 2015). Although the effects of CART on the body may be by directly or indirectly affecting the cells, it is not known how these peptides exert their effects on cells. This is largely because CART specific receptors have not yet been identified. Therefore, their exact cellular mechanisms and consequences are not known.

Nevertheless, some CART binding and signaling studies have been carried out. In one study, voltage dependent intracellular calcium signaling was inhibited by CART 55-102 (Yermolaieva et al., 2001). In another, it was found that CART 55-102 induced a dose and time dependent activation of p-ERK 1 and 2. Moreover, when the effect of CART 55-102 was blocked by inhibitors such as genistein and pertussis toxin, it was indicated that the upstream kinases MEK1 and 2 were involved into the signal pathway. Therefore, the presence of a Gi/Go coupled G protein coupled receptor (GPCR) involved in CART 55-102 signaling was considered (Lakatos et al., 2005).

Radiolabeled CART peptides and different CART peptide fragments were created to discover any binding. However, there was no specific binding or specific blockage by CART peptide fragments. Many publications supported these observations (Lin et al., 2011).

Considering all the functions of CART peptides and the lack of a specific receptor, identification of the CART receptor has a high priority to understand the molecular and cellular pathways of CART. Therefore, our aim was to identify potential candidate CART receptors. To specify candidate genes and to do related signaling experiments, we benefited from a previous study from our group. Twelve different CART receptor genes were selected by analyzing online published microarray data (Merve Kasap, M.Sc thesis, 2014, METU Biological Sciences, Ankara). In the microarray study, HEK293, N18, AtT20, and BV2 cell lines were used (Atwood et al., 2011). AtT-20 was found to response to CART peptide. However, the N2a cell line was nonresponsive to CART. Therefore, the AtT20 cell line was used for expression studies. Gi/Go coupled GPCR has been suggested as the primary receptor for the CART signaling (Lakatos et al., 2005). Thus, 12 candidate CART receptor genes were selected among orphan GPCRs that were expressed in AtT20 cell line. To verify their expression levels, q-RT-PCR experiments were done for 12 genes (*BAI1, BAI3, CASR, CRHR1, Fzd10, GLP1R, GLP2R, GPR113, GPR116, GPR133, GRM1* and *SCTR*) and 7 of them were found to be promising to be highly expressed in the AtT-20 cell line and determined candidate CART receptor genes. These genes were *SCTR, GRM1, GLP1R, GLP2R, CASR, GLP133* and *GLP116.*

These selected 7 candidate GPCR genes were known to have different roles in cells. SCTR (secretin receptor) binds to secretin and regulates pancreatic function and secretion. It is also known to be involved in pancreatic cancer and autism. CASR (calcium sensing receptor) regulates calcium ions changes and maintains calcium homeostasis in cells. GRM1 (glutamate metabotropic receptor) activates phospholipase C and is activated by L-glutamate which is an excitatory

neurotransmitter. This gene might be associated with schizophrenia, bipolar disorder, depression and breast cancer. GLP1R (glucagon like peptide 1 receptor) stimulates glucose-induced insulin secretion, protects neurons and is associated with diabetes. GLP2R (glucagon like peptide 2 receptor) is related to the glucagon receptor, stimulates intestinal growth and increases villus height in the small intestine and decreases enterocyte apoptosis. GPR133 (adhesion G protein-coupled receptor D1) is a membrane-bound protein and associated with hypoxia and tumor growth in glioblastoma (GBM). GPR116 (adhesion G protein-coupled receptor F5) regulate acid-base balance and is involved in embryonic development, immune response and breast cancer.

In this study, we aimed to verify those previously detected 7 different candidate CART receptor genes using TANGO vectors. For this purpose, genes were digested with the NotI enzyme to check the sizes of genes and compared with undigested ones. On agarose gels, two faint bands were detected for the 5 undigested genes other than GPR116 and SCTR plasmid DNAs which were supercoiled and nicked DNA from undigested DNAs. Multiple copies of DNA of fixed length were not seen in the undigested DNAs. Since the undigested sample was a mixture of DNA fragment sizes and long lysis step (alkaline conditions) of plasmid isolation gave single stranded closed circles, the expected size of the 5 different genes could not be detected because of improper restriction digestion (Wheeler et al., 1992) and consistently, two separate bands were detected.

To detect the SCTR gene, a PCR protocol was performed for old and new SCTR genes. There was no band for the PCR product of *SCTR* using the new plasmid DNAs. Therefore, new colonies were selected from agar plates to isolate new plasmid DNAs and these plasmid DNAs were shown to be accurate in size within TANGO vectors. Nevertheless, when the PCR was carried out for the new SCTR genes, SCTR gene amplification could not be detected for the new plasmids. Even when the next generation sequencing was performed for SCTR, it could not be detected in the TANGO vectors. However, using new primers for all genes, the size

of the genes was found to be larger than their actual insert size. This was due to additional sequences came from the TetR gene. The sequencing result of *GLP1R* and *GLP2R* indicated that these two genes were present in the TANGO vectors and due to additional sequences from the TetR gene, higher band sizes were detected.

After presence of putative CART receptor genes was detected in the PCR results, plasmid DNAs were transfected into N2a cells. After transfection, cells that were stimulated with CART 62-102 were analyzed for anti-p-ERK 1/2 by using Western Blot. According to our hypothesis, these candidate genes may increase p-ERK through CART receptor/s.

Based on our results, activation of p-ERK 1/2 could not be detected for any of the genes. Only transfection of the GLP1R gene may have generated a slight increase in p-ERK 1/2 when compared to unstimulated *GLP1R* transfected N2a cells. This needs further investigations to investigate the possibility of *GLP1R* as a potential candidate.

For future studies, the remaining 5 other candidate genes may be sequenced. Different concentrations of CART (10 µM, 5 µM, 2 µM, 1 µM, 0,5 µM, 100 nM, 10 nM, 1 nM, even 1000 femtoM, 100 femtoM, 10 femtoM) may be examined using different time intervals (10, 5, 2, 1 min.) and also using different cell lines for p-ERK 1/2 response.

In addition, different cellular pathways might also be analyzed for CART response. For instance, besides activating the MEK and ERK pathways, CART peptide also induces c-fos expression, used as a marker for neuronal activity, might be investigated in neurons. CART also increases phosphorylation of CREB (p-CREB) and expression of early growth response 1 (EGR-1) in hypothalamus and brain stem neurons which regulate CART expression; therefore, change of their level may provide some evidence about CART signaling. Therefore, c-fos, p-CREB, cAMP and PKA levels may also be investigated using different conditions to evaluate possible CART receptor response.

CHAPTER 5

CONCLUSIONS

Our previous microarray analysis revealed that seven candidate CART receptor genes may encode potential CART receptors. In this study, we attempted to transfect these candidate genes into a nonresponsive cell line, N2a and following stimulation of the cells with CART 62-102 to detect p-ERK 1 and 2 responses by Western Blot using anti-p-ERK 1/2. Therefore, after transfection of N2a, cells were treated with 10 μM CART 62-102 for 5 and 10 minutes and then total proteins were collected. HEK293 cell line was used as a positive control for p-ERK 1/2 response.

In our results, there was a slight increase in p-ERK 1/2 for GLP1R gene when cells were treated for 5 min with CART compared to unstimulated *GLP1R* transfected N2a cell just once. Even though several attempts were carried out with GLP1R transfection, we were not able to repeat the same positive response of p-ERK in the cells. Next, all cells that were transfected with 7 different genes were treated with CART for 10 min and 5 min, but no p-ERK 1/2 response could be detected.

In conclusion, after CART stimulation, p-ERK 1/2 could not be detected in our transfected cells for any of genes. Nevertheless, different approaches may be taken to analyze the CART response when the cells are transfected with these candidate genes. Such as cAMP, p-CREB, PKA levels may be investigated besides p-ERK 1/2 response. Also, these cells may be stimulated with different concentrations of CART 62-102 and CART 55-102 for different time intervals.

REFERENCES

Abbott et al., 2001. *Evidence of an orexigenic role for cocaine- and amphetamine-regulated transcript after administration into discrete hypothalamic nuclei.* Endocrinology. 142:3457–3463.

Abels et al., 2016. *CART is overexpressed in human type 2 diabetic islets and inhibits glucagon secretion and increases insulin secretion.* Diabetologia. September 2016, Volume 59, Issue 9, pp 1928–1937.

Ahima et al., 1998. *Leptin activates hypothalamic CART neurons projecting to the spinal cord.* Neuron. 21 (1998), pp. 1375-1385.

Aja et al., 2001. *Intracerebroventricular CART peptide reduces rat ingestive behavior and alters licking microstructure.* Am J Physiol. 280:R1613–R1619.

Ashish et al., 2016. *Pro-cognitive action of CART is mediated via ERK in the hippocampus: Role of CART in recognition memory*. Hippocampus 26(10) · June 2016.

Atwood et al., 2011. *Expression of G protein-coupled receptors and related proteins in HEK293, AtT20, BV2, and N18 cell lines as revealed by microarray analysis.* BMC Genomics 201112:14.

Baharne et al., 2016. *Pro-cognitive action of CART is mediated via ERK in the hippocampus.* Hippocampus. Volume26, Issue10 October 2016. Pages 1313-1327.

Bakhtazad et al., 2016. *Evaluation of CART peptide level in rat plasma and CSF: Possible role as a biomarker in opioid addiction.* Peptides. Volume 84, Pages 1-6.

Bakhtazad et al., 2017. *Evaluation of the CART peptide expression in morphine sensitization in male rats.* European Journal of Pharmacology. Volume 802, 5 May 2017, Pages 52-59.

Blechova et al., 2013. *New analogs of the CART peptide with anorexigenic potency: the importance of individual disulfide bridges*. Peptides. 2013:138-44.

Broberger 1999. *Hypothalamic cocaine- and amphetamine-regulated transcript (CART) neurons: histochemical relationship to thyrotropin-releasing hormone, melanin-concentrating hormone, orexin/hypocretin and neuropeptide Y.* Brain Res. 848:101–113.

Butera 2010. *Estradiol and the control of food intake*. Physiol Behav, 99 (2010), pp. 175-180.

Coopman et al., 2010. *Comparative effects of the endogenous agonist glucagon-like peptide-1 (GLP-1)-(7-36) amide and the small-molecule ago-allosteric agent "compound 2" at the GLP-1 receptor.* J Pharmacol Exp Ther. 2010 Sep 1;334(3):795-808.

Cota et al., 2003. *The endogenous cannabinoid system affects energy balance via central orexigenic drive and peripheral lipogenesis.* J Clin Investig. 112:423– 431.

Couceyro et al., 2005. *Cocaine- and amphetamineregulated transcript (CART) peptides modulate the locomotor and motivational properties of psychostimulants*. J Pharmacol Exp Ther 315:1091–1100.

Dallvechia-Adams et al., 2002. *Cocaine- and amphetamine-regulated transcript peptide projections in the ventral midbrain: colocalization with gamma-aminobutyric acid, melanin-concentrating hormone, dynorphin, and synaptic interactions with dopamine neurons.* J Comp Neurol. 2002 Jul 8;448(4):360-72

Daly 1996. *Influence of acute and chronic morphine or stadol on the secretion of adrenocorticotrophin and its hypothalamic releasing hormone in the rat.* Life Sci. 1996;59(22):1881-90.

Dandekar et al., 2012. *Involvement of CART in estradiol-induced anorexia*. Physiology & Behavior. Volume 105, Issue 2, 18 January 2012, Pages 460–469.

Dauer et al., 2003. *Parkinson's disease: mechanisms and models*. Neuron. 2003 Sep 11;39(6):889-909.

De Foubert et al., 2004. *Fluoxetine-induced change in rat brain expression of brain-derived neurotrophic factor varies depending on length of treatment*. Neuroscience. 2004;128(3):597-604.

del Giudice et al., 2001. *Mutational screening of the CART gene in obese children: identifying a mutation (Leu34Phe) associated with reduced resting energy expenditure and cosegregating with obesity phenotype in a large family.* Diabetes 50, 2157–2160 10.2337/diabetes.50.9.2157

Dominguez et al., 2002. *Characterization of the cocaine- and amphetamine-regulated transcript (CART) peptide gene promoter and its activation by a cyclic AMP-dependent signaling pathway in GH3 cells*. Journal of Neurochemistry. 2002

Dominguez et al., 2004. *CART peptide levels are altered by a mutation associated with obesity at codon 34.* Mol. Psychiatry 9, 1065–1066

Douglass et al., 1995. *PCR differential display identifies a rat brain mRNA that is transcriptionally regulated by cocaine and amphetamine.* J Neurosci. 1995 Mar; 15(3 Pt 2): 2471-81.

Dun et al., 2000. *Differential expression of cocaine- and amphetamine-regulated transcript-immunoreactivity in the rat spinal preganglionic nuclei.* Neurosci Lett. 294:143–146.

Dylag et al., 2006. *CART (85–102)—Inhibition of psychostimulant-induced hyperlocomotion: Importance of cyclization.* Peptides. Pages 3183-3192.

Egemen et al., 2016. *Nicotine regulates cocaine-amphetamine-Regulated Transcript (Cart) in the mesocorticolimbic system.* Synapse. 14 March 2016.

Elmquist et al., 1999. *From lesions to leptin: hypothalamic control of food intake and body weight.* Neuron 22:221–232.

Folger et al., 2009. *Evidence supporting a role for cocaine and amphetamine regulated transcript (CART) in control of granulosa cell estradiol production associated with dominant follicle selection in cattle.* Biol Reprod. 2009;81(3):580–586.

Garcia Luna et al., 2017. *Impaired hypothalamic cocaine- and amphetamine-regulated transcript expression in lateral hypothalamic area and paraventricular nuclei of dehydration-induced anorexic rats.* J Neuroendocrinol. 2017 Nov;29(11).

Hendolin et al., 2003. *Activation of the TrkB Neurotrophin Receptor Is Induced by Antidepressant Drugs and Is Required for Antidepressant-Induced Behavioral Effects.* Journal of Neuroscience 1 January 2003, 23 (1) 349-357.

Holsboer et al., 2008. *Central CRH system in depression and anxiety--evidence from clinical studies with CRH1 receptor antagonists*. Eur. J. Pharmacol. 2008;583:350–357.

Hunter et al., 2005. *The effects of cocaine on CART expression in the rat nucleus accumbens: a possible role for corticosterone*. Eur J Pharmacol. 2005;517:45–50.

Janhunen et al., 2004. *Comparison of the effects of nicotine and epibatidine on the striatal extracellular dopamine.* European Journal of Pharmacology. 2004, 494(2-3):167-77

Jaworski et al., 2003. *Intra-accumbal injection of CART (cocaine-amphetamine-regulated transcript) peptide reduces cocaineinduced locomotor activity*. J Pharmacol Exp Ther 307:1038 –1044.

Jaworski et al., 2008. *Injection of CART (cocaine- and amphetamine-regulated transcript) peptide into the nucleus accumbens reduces cocaine self-administration in rats*. Behav. Brain Res. 2008;191:266–271.

Jensen et al., 1999. *The hypothalamic satiety peptide CART is expressed in anorectic and non-anorectic pancreatic islet tumors and in the normal islet of Langerhans.* FEBS Lett. 447:139 –143.

Jiao et al., 2018. *CART peptide activates the Nrf2/HO-1 antioxidant pathway and protects hippocampal neurons in a rat model of Alzheimer's disease*. Biochem Biophys Res Commun. 2018 Jul 2; 501(4):1016-1022.

Jin JL et al., 2015. *CART treatment improves memory and synaptic structure in APP/PS1 mice*, Sci Rep. 2015 May 11;5:10224.

Jin et al., 2015. *CART treatment improves memory and synaptic structure in APP/PS1 mice.* Scientific Reports volume5, Article number: 10224.

Job et al., 2011. *CART Peptides Regulate Psychostimulants and May be Endogenous Antidepressants.* Curr Neuropharmacol. 2011 Mar; 9(1): 12–16.

Jones et al., 2006. *Cocaine-amphetamine-regulated transcript expression in the rat nucleus accumbens is regulated by adenylyl cyclase and the cyclic adenosine 5'-monophosphate/protein kinase a second messenger system.* J Pharmacol Exp Ther. 2006 Apr;317(1):454-61.

Jung et al., 2004. *Association between polymorphism in intron 1 of cocaine- and amphetamine-regulated transcript gene with alcoholism, but not with bipolar*

disorder and schizophrenia in Korean population. Neurosci Lett. 2004;365:54–57.

Kelly et al., 2005. *Activation of mitogen-activated protein kinase/extracellular signal-regulated kinase in hippocampal circuitry is required for consolidation and reconsolidation of recognition memory.* J. Neurosci. 2003;12:5354–5360.

Kimmel et al., 2000. *Intra-ventral tegmental area injection of rat cocaine and amphetamine-regulated transcript peptide 55–102 induces locomotor activity and promotes conditioned place preference*. J Pharmacol Exp Ther 294:784 – 792.

Kller PA, et al. *Characterization and localization of cocaine- and amphetamine-regulated transcript (CART) binding sites*. Peptides. 2006;27:1328–1334.

Koob et al., 2005. *Plasticity of reward neurocircuitry and the 'dark side' of drug addiction.* Nat Neurosci. 2005;8:1442–1444.

Koylu et al., 1997. *Immunohistochemical localization of novel CART peptides in rat hypothalamus, pituitary and adrenal gland.* J Neuroendocrinol. 1997 Nov;9(11):823-33.

Koylu et al., 1998. *Cocaine- and amphetamine-regulated transcript peptide immunohistochemical localization in the rat brain.* J Comp Neurol. 391:115–132.

Kristensen et al., 1998. *Hypothalamic CART is a new anorectic peptide regulated by leptin.* Nature, 393 (1998), pp. 72-76.

Kroeze et al., *2015. PRESTO-Tango as an open-source resource for interrogation of the druggable human GPCRome.* Nat Struct Mol Biol. 2015 May;22(5):362-9.

Kuhar et al., 1999. *CART peptide-immunoreactive neurones in the nucleus accumbens in monkeys: ultrastructural analysis, colocalization studies, and synaptic interactions with dopaminergic afferents.* J Comp Neurol. 407:491–511.

Kuhar et al., 2002. *CART Peptides*. Neuropeptides. 2002 Feb;36(1):1-8.

Kuhar 2016. *CART Peptides and Drugs of Abuse: A Review of Recent Progress.* Journal of Drug and Alcohol Research. Vol. 5 (2016)

Lakatos et al., 2005. *Cocaine- and amphetamine-regulated transcript (CART) peptide activates the extracellular signal-regulated kinase (ERK) pathway in AtT20 cells via putative G-protein coupled receptors*. Neurosci Lett. 2005 Aug 12-19;384(1-2):198-202.

Lambert et al., 1998. *CART peptides in the central control of feeding and interactions with neuropeptide Y.* Synapse. 29:293–298

Larsen et al., 2000. *Chronic intracerebroventricular administration of recombinant CART(42– 89) peptide inhibits and causes weight loss in lean and obese Zucker (fa/fa) rats.* Obes Res. 8:590 –596

Lin et al., 2011. *CART Peptide Stimulation of G Protein-Mediated Signaling in Differentiated PC12 Cells: Identification of PACAP 6-38 as a CART Receptor Antagonist.* Neuropeptides. 2011 Oct; 45(5): 351–358

Ma et al., 2007. *CART peptides increase 5-hydroxytryptamine in the dorsal raphe and nucleus accumbens of freely behaving rats*. Neurosci Lett. 2007;417:303–307

Ma et al., 2016. *Leptin-Induced CART (Cocaine- and Amphetamine-Regulated Transcript) Is a Novel Intraovarian Mediator of Obesity-Related Infertility in Females.* Endocrinology. 2016 Mar; 157(3): 1248–1257

Makowska et al., 2018. *Cocaine- and amphetamine-regulated transcript (CART) peptide in the enteric nervous system of the porcine esophagus.* C R Biol. 2018 Jul - Aug;341(6):325-333.

Matsumura et al., 2001. *Central human cocaine- and amphetamine-regulated transcript peptide 55–102 increases arterial pressure in conscious rabbits.* Hypertension. 38:1096 –1100.

Matsumura, et al., 2015. *Central human cocaine- and amphetamine- regulated transcript peptide 55–102 increases arterial pressure conscious rabbits*. Hypertension (2015), pp. 1096-1101.

Mattsont al., 2005. *Preference for cocaine- versus pup-associated cues differentially activates neurons expressing either Fos or cocaine- and amphetamineregulated transcript in lactating, maternal rodents.* Neuroscience 135:315–328.

Moffett et al., 2011. *CART peptide inhibits locomotor activity induced by simultaneous stimulation of D1 and D2 receptors, but not by stimulation of individual dopamine receptors.* Synapse, 65 (1).

Muñoz-Rodríguez et al., 2018. *Cocaine and amphetamine regulated transcript and brain-derived neurotrophic factor in morbid obesity. One-year follow-up after gastric bypass.* Surg Obes Relat Dis. 2018 Jul 31. pii: S1550-7289(18)30452-0.

Nauck et al., 1993. *Preserved incretin activity of glucagon-like peptide 1 [7-36 amide] but not of synthetic human gastric inhibitory polypeptide in patients with type-2 diabetes mellitus.* J Clin Invest. 1993 Jan;91(1):301-7

Palus et al., 2018. *Acrylamide-induced alterations in the cocaine- and amphetamine-regulated peptide transcript (CART)-like immunoreactivity within the enteric nervous system of the porcine small intestines.* Ann Anat. 2018 Sep;219:94-101

Pierce et al., 2006. *The mesolimbic dopamine system: the final common pathway for the reinforcing effect of drugs of abuse?.* Neurosci Biobehav Rev. 2006;30(2):215-38. Epub 2005 Aug 11.

Rale et al., 2017. *CART neuropeptide modulates the extended amygdalar CeA-vBNST circuit to gate expression of innate fear*. Psychoneuroendocrinology. 2017 Nov;85:69-77.

Rogge et al., 2008. *CART peptides: regulators of body weight, reward and other functions.* The Journal of Pharmacology and Experımental Therapeutıcs. Nat Rev Neurosci. 2008 Oct; 9(10): 747–758.

Rohner-Jeanrenaud et al., 2002. *Chronic central infusion of cocaine- and amphetamine-regulated transcript (CART 55–102): effects on body weight homeostasis in lean and high-fat-fed obese rats.* Int J Obes Relat Metab Disord. 26:143–149.

Romeu et al., 2018. *Central action of CART induces neuronal activation in the paraventricular and dorsomedial hypothalamus of diet-induced obese and lean mice*. Neurosci Lett. 2018.

Salinas et al., 2006. *Ethanol enhancement of cocaine- and amphetamine-regulated transcript mRNA and peptide expression in the nucleus accumbens*. J Neurochem. 2006;97: 408–415

Sarkar et al., 2004. *Central administration of cocaine- and amphetamine-regulated transcript increases phosphorylation of cAMP response element binding protein in corticotropin-releasing hormoneproducing neurons but not in prothyrotropin-releasing hormone-producing neurons in the hypothalamic paraventricular nucleus.* Brain Res. 999:181–192.

Sathanoori et al., 2013. *Cocaine- and Amphetamine-regulated Transcript (CART) Protects Beta Cells against Glucotoxicity and Increases Cell Proliferation*. J Biol Chem. 2013 Feb 1; 288(5): 3208–3218.

Silva et al., 2010. *EliasEstradiol-induced hypophagia is associated with the differential mRNA expression of hypothalamic neuropeptides.* Braz J Med Biol Res, 43 (2010), pp. 759-766.

Smith et al., 1999. *CART peptide-immunoreactive neurones in the nucleus accumbens in monkeys: ultrastructural analysis, colocalization studies, and synaptic interactions with dopaminergic afferents*. J. Comp. Neurol. 407, 491–511.

Stein et al., 2006. *Processing of cocaine- and amphetamine-regulated transcript (CART) precursor proteins by prohormone convertases (PCs) and its implications.* Peptides. 2006 Aug; 27(8):1919-25.

Stein et al., 2006. *Processing of cocaine- and amphetamine-regulated transcript (CART) precursor proteins by prohormone convertases (PCs) and its implications*. Peptides. 2006 Aug;27(8):1919-25.

Subhedar et al., 2016. *CART modulates the effects of levodopa in rat model of Parkinson's disease.* Behavioural brain research 301:262-272.

Szuba et al., 2005. *Rapid antidepressant response after nocturnal TRH administration in patients with bipolar type I and bipolar type II major depression.* J Clin Psychopharmacol. 2005 Aug;25(4):325-30.

Tang et al., 2003. *Molecular profiling of midbrain dopamine regions in cocaine overdose victims.* J Neurochem 85:911–924.

Thim et al., 1998. *Purification and characterisation of a new hypothalamic satiety peptide, cocaine and amphetamine regulated transcript (CART), produced in yeast.* FEBS Lett. 1998 May 29; 428(3):263-8.

Thim et al., 1999. *Tissue-specific processing of cocaine- and amphetamine-regulated transcript peptides in the rat.* Proc Natl Acad Sci U S A. 1999 Mar 16; 96(6):2722-7.

Tian et al., 2004. *Changes of hypothalamic alpha-MSH and CART peptide expression in diet-induced obese rats.* Peptides. 2004;25:2147–53.

Tsuruta et al., 2002. *Hyperleptinemia in A y /a mice upregulates arcuate cocaine- and amphetamine-regulated transcript expression*. AJP Endocrinology and Metabolism.

Upadhya et al., 2011. *Cocaine- and amphetamine-regulated transcript peptide increases spatial learning and memory in rats*. Life Sci. 2011 Feb 14;88(7-8):322-34.

Upadhya et al., 2012. *CART peptide in the nucleus accumbens shell acts downstream to dopamine and mediates the reward and reinforcement actions of morphine.* Neuropharmacology. 2012 Mar;62(4):1823-33.

Upadhya et al., 2016. *CART modulates the effects of levodopa in rat model of Parkinson's disease.* Behavioural Brain Research, Volume 301, 2016, Pages 262–272.

Venancio et al., 2017. *Short-Term High-Fat Diet Increases Leptin Activation of CART Neurons and Advances Puberty in Female Mice.* Endocrinology. 2017 Nov 1;158(11):3929-3942.

Vicentic et al., 2006. *The CART (Cocaine- and Amphetamine-Regulated Transcript) System in Appetite and Drug Addiction.* Division of Neuroscience.

Vicentic et al., 2006. *The CART receptors: Background and recent advances.* Peptides.

Vicentic et al., 2007. *The CART (cocaine- and amphetamine-regulated transcript) system in appetite and drug addiction.* J Pharmacol Exp Ther. 2007 Feb;320(2):499-506.

Vrang et al., 1999. *Neurochemical characterization of hypothalamic cocaine-amphetamine-regulated transcript neurons*. J Neurosci. 19:RC5.

Yang et al., 2005. *Cocaine- and amphetamine-regulated transcript in the nucleus accumbens participates in the regulation of feeding behavior in rats.* Neuroscience. 133:841– 851.

Yanik et al., 2006. *The Leu34Phe Procart Mutation Leads to Cocaine and Amphetamine Regulated Transcript (CART) Deficiency: A Possible Cause for Obesity in Humans.* Endocrinology, Volume 147, ıssue 1, 1 January 2006, pages 39–43.

Yao et al., 2004. *Evidence that cocaine- and amphetamine-regulated transcript is a novel intra-ovarian regulator of follicular atresia*. Endocrinology. 2004;145(11):5373–5383.

Yermolaieva et al., 2001. *Cocaine- and Amphetamine-Regulated Transcript Peptide Modulation of Voltage-Gated Ca2 Signaling in Hippocampal Neurons*. The Journal of Neuroscience. October 1, 2001, 21(19):7474–7480.

Zain et al., 2008. *Impact of Obesity on Female Fertility and Fertility Treatment.* Womens Health (Lond). 2008Mar;4(2):183-94.

Zhu et al.,2018. *RANKL Reduces Body Weight and Food Intake via the Modulation of Hypothalamic NPY/CART Expression*. Int J Med Sci. 2018; 15(10): 969–977.

Wheeler et al., 1992. *Distinction between supercoiled and linear DNA in transverse agarose pore gradient gel electrophoresis.* Electrophoresis. 1992 Jul;13(7):403-6.

Wierup et al., 2006. *CART regulates islet hormone secretion and is expressed in the beta-cells of type 2 diabetic rats.* Diabetes. 55:305–311.

William et al., 1997. *Effect of pH and Ionic Strength on the Spectrophotometric Assessment of Nucleic Acid Purity*. BioTechniques 22:474-481 (March 1997)

Wortley et al., 2004. *Cocaine- and amphetamine-regulated transcript in the arcuate nucleus stimulates lipid metabolism to control body fat accrual on a high-fat diet.* Regul. Pept. 117, 89–99

APPENDICES

A. NANODROP RESULTS FOR PLASMİD DNAs

Table A.1: Nanodrop Results of SCTR, CASR and GPR116 Plasmid DNAs

	A 260/280	**A 260/230**	**µg/ul**
SCTR 1 (new)	1.940	2.365	0.097
SCTR 2 (new)	1.933	1.999	0.118
SCTR 3 (new)	1.961	1.747	0.096
CASR 1	1.958	2.174	0.119
CASR 2	1.897	2.253	0.264
CASR 3	1.950	2.262	0.142
Gpr116 -1	2.041	2.183	0.063
Gpr116-2	1.985	1.687	0.079
Gpr116-3	2.015	2.346	0.071

Table A.2. Nanodrop Results of GLP2R, GLP1R and GRM1 Plasmid DNAs

	A 260/280	**A 260/230**	**µg/ul**
GLP2R-1	1.883	2.252	0.241
GLP2R-2	1.880	2.254	0.261
GLP2R-3	1.896	2.203	0.258
GLP1R-1	1.922	2.267	0.204
GLP1R-2	1.877	2.235	0.360
GLP1R-3	1.878	2.311	0.411
GRM1-1	1.913	2.311	0.203
GRM1-2	1.935	2.149	0.207
GRM1-3	1.922	2.249	0.225

Table A.3. Nanodrop Result of old SCTR, old CRHR1 and GPR133 Plasmid DNAs

	A 260/280	**A 260/230**	**µg/ul**
SCTR-1 (old)	1.881	2.244	0.290
SCTR-2 (old)	1.894	2.537	0.314
SCTR-3 (old)	1.905	2.212	0.234
CRHR1-1 (old)	1.905	1.676	0.139
CRHR1-2 (old)	1.896	2.075	0.110
CRHR1-3 (old)	1.931	2.302	0.108
GPR133-1	1.982	2.626	0.048
GPR133-2	1.899	2.194	0.241
GPR133-3	1.893	2.611	0.220

B. TABLES OF MATERIALS FOR PCR

Table B.1. *SCTR* Gradient PCR Reagents

Reagents	Volume/ PCR tubes
10 X PCR Buffer	5 µl
10 mM dntp mix	1 µl
Forward Primers	2.5 µl
Reverse Primers	2.5 µl
25 mM $MgCl_2$	4 µl
DNA	2 µl
Taq Polymerase	0.25 µl
Nuclease Free Water	32.75 µl
Total	50 µl

Table B.2. Thermal Cycler Protocol for PCR

Protocol Steps	Temperature	Duration
Initial Denaturation	94°C	2 min
Denaturation	94°C	30 secs
Annealing	64°C	30 secs
Extension	74°C	2 min
Final Extension	74°C	5 min
Incubation	4°C	Indefinitely

Table B.3. Primer Sequences of SCTR Gene

Forward Primer: 5’ GTTGTTGTTGCTAGCATGCGTCCCCACCTGTCGC 3’
Reverse Primer: 5’ GTTGTTGTTGAATTCTCAGATGATGCTGGTCCTGC 3’

Table B.4: Sequences of TANGO Vector Forward and Reverse Primers

T7 Forward Primer	5’ TAATACGACTCACTATAGGG 3’
BGH Reverse Primer	5’ TAGAAGGCACAGTCGAGG 3’

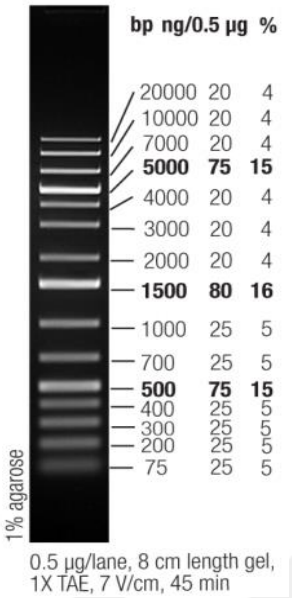

Figure B.1: DNA Ladder: O'GeneRuler 1 kb Plus DNA Ladder

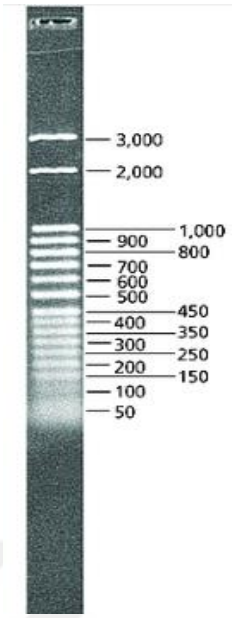

Figure B.2: DNA Ladder: DirectLoad^{TM} 50 bp DNA Step Ladder

C. COMPLETE CELL MEDIUM PROTOCOL

C.1 Complete Cell Medium Contents;

a. 445 mL DMEM (Classical Cell Culture Medium, Biological Industries, Cromwell CT, USA)

b. 50 mL FBS (Fetal Bovine Serum, Biological Industries, Cromwell CT, USA)

c. 5.5 mL L-Gluthamine (Biological Industries, Cromwell CT, USA)

d. 0.5 mL Penicillin/ Streptomycine (10.000 µg/mL stock solution) (Biochrom, Berlin, Germany)

C.2 After these contents were mixed in a 500 mL Filter System (Corning, NY,USA), the mixture was filtered by the help of vacuum machine under the hood and kept at 4°C. It was pre-warmed in a 37°C water bath before adding to the cells.

C.3 Cell culture maintenance was achieved by adding 5% DMSO to the complete medium. Then cells were kept at -80°C overnight and transferred to nitrogen vapor phase for long time storage.

D. TOTAL PROTEIN CONCENTRATIONS OF CELLS (µg/ul)

Table D.1. HEK293 cell protein concentration (µg/ul)

HEK293
5.55

Table D.2. N2a cell protein concentrations (µg/ul) ("Trans." means transfected, "-means; there was no CART stimulation, "+" means; there was CART stimulation) for Western Blot 1

No Transfection -	**No transfection +**	**HEK293 cell proteins**	***CASR* Trans. -**
9.9	6.4	9.5	10.1
***CASR* Trans. +**	***SCTR* Trans. -**	***SCTR* Trans. +**	***GRM1* Trans. -**
9.6	7.07	6.8	9.1
***GRM1* Trans. +**	***GPR116* Trans. -**	***GPR116* Trans. +**	***GLP2R* Trans. -**
6.29	7.02	6.33	9.54
***GLP2R* Trans. +**	***GLP1R* Trans. -**	***GLP1R* Trans. +**	***GPR133* Trans. -**
9.9	7.2	9.7	6
***GPR133* Trans. +**			
6.65			

Table D.3. N2a cell protein concentrations (µg/ul) ("Trans." means transfected, "-means; there was no CART situmulation, "+" means; there was CART stimulation) for Western Blot 2

No Transfection -	**No Transfection +**	**HEK293 cell proteins**	***CASR* Trans. -**
0.85	0.7	0.31	0.14
***CASR* Trans. +**	***SCTR* Trans. -**	***SCTR* Trans. +**	***GRM1* Trans. -**
0.3	0.33	0.35	0.17
***GRM1* Trans. +**	***GPR116* Trans. -**	***GPR116* Trans. +**	***GLP2R* Trans. -**
0.48	0.13	0.4	0.36
***GLP2R* Trans. +**	***GLP1R* Trans. -**	***GLP1R* Trans. +**	***GPR133* Trans. -**
0.49	0.31	0.44	1.6
***GPR133* Trans. +**			
1			

E. TABLES OF MATERIALS FOR WESTERN BLOT

Table E.1. SDS-PAGE Gel Materials

	10% Separating Gel for 2 gels (volume)	**4% Stacking Gel for 2 gels (volume)**
dH_2O	6 mL	3 mL
Acr/ Bis (30%)	5 mL	650 µl
1.5 M Tris-HCl (ph: 8.8)	3.8 mL	
0.5 M Tris-HCl (ph: 6.8)		1.25 mL
10% SDS	75 µl	25 µl
10% APS	100 µl	100 µl
TEMED	10 µl	10 µl

Table E.2. 4X Tris-Cl/SDS (pH 8.8)

Tris base	18.2 g
SDS	0.4 g
H_2O	to 100 mL

pH adjusted with HCl or NaOH and stored at 4ºC.

Table E.3. 4X Tris-Cl/SDS (pH 6.8)

Tris base	3.02 g
SDS	0.2 g
H_2O	to 50 mL

pH adjusted with HCl or NaOH and stored at 4ºC.

Table E.4. 30% / 8% (w/v) Acrylamide Bisacrylamide

Acrylamide	30 gr
Bisacrylamide	0.8 gr
H_2O	to 100 ml

Stored at 4ºC and protected from the light.

Table E.5. 10% APS

APS	1.0 g
H_2O	to 10 mL

Dissolved and aliquoted then stored at -20ºC.

Table E.6. Coomassie Staining Buffer

Coomassie Brilliant Blue Reagent	2.5 g
Methanol (40%)	400 mL
H_2O	530 mL
Acetic acid (7% at last)	70 mL

First, methanol and Coomassie BBR were mixed and acetic acid and water were mixed separately. Then they were mixed together and filtered. In a bottle, the solution was stored at room temperature for up to 2 months.

Table E.7. Coomassie Destaining Buffer

Methanol	200 mL
Acetic acid	200 mL
Isopropanol	200 mL
H_2O	to 2000 mL

Solution was stored at room temperature.

Table E.8. 4X sample buffer for reducing conditions

125m M Tris-Cl, pH 6.8	3.2 mL
Glycerol 40%	4 mL
SDS 8%	0.8 g
2-Mercaptoethanol 20%	2.0 mL
Bromophenol blue 0.02%	2 mg
H_2O	to 10 mL

Solution was aliquoted and stored at -20°C.

Table E.9. 10X Electrophoresis Running buffer (pH 8.3)

Tris base	30 g
SDS	10 g
Glycine	144 g
H_2O	to 1L

Solution was diluted to 1X before usage. pH was adjusted with HCl to 8.3 and stored at room temperature.

Table E.10. 10X Transfer buffer

Tris base	30 g
Glycine	144 g
H_2O	to 1L

Mixed and stored at 4°C. Solution was diluted to 1X before usage.

Table E. 11. 10X TBS (pH 7.4)

Tris base	24.0 gr
NaCl	88.0 gr
H_2O	to1 L

pH was adjusted with HCl/NaOH to 7.4 and stored at room temperature and solution was diluted to 1X before usage.

Table E. 12. 1X Tween TBS (T-TBS)

1 X TBS	500 mL
20% Tween	0.5 mL

Mixed and stored at room temperature.

Table E. 13. 3% Blocking Solution

Milk powder	3 g
1X TBS-T	to 100 Ml

Prepared freshly before use.

Table E. 14. Mild Stripping Solution

Glycine	3 gr
SDS	0.2 gr
Tween 20	2 mL
H_2O	to 200 mL

Adjust pH with HCl/NaOH to 2.2 on stirrer and stored for 3 or 4 days at room temperature.

Table E. 15. 0.05 % Tween 20 in TBS

1X TBS	500 mL
20 % Tween 20	250 µl

Mixed on a stirrer and stored at room temperature.

Table E.16. Dilution Rates of p-ERK1/2 Antibody

Dilution Rates	Required p-ERK1/2 amount (µl)
1/ 1000	10 µl
1/2000	5 µl
1/5000	2 µl
1/10000	1 µl

F. p-ERK 1/2 WESTERN BLOT PROCEDURE

F.1 SDS gels were prepared according to Appendix E.1.

F.2 Protein samples were prepared by mixing them with 4X loading buffer.

F.3 Gel apparatus was placed in buffer tank and tank was filled with 1X Running Buffer and gels were assembled into gel apparatus. For these experiments, 2 gels were used. Then, 50 µg protein samples were loaded to the SDS-PAGE gels using micropipette.

F.4 Gels were run at 110 Volt until protein ladder reached to the end of the gel.

F.5 Meanwhile, PVDF membrane was cut at 8x6 cm dimensions. Two membranes were cut for two gels. Both membranes were soaked with methanol for 30 secs and then with 1X transfer buffer for 15 minutes. At the same time, transfer materials were prepared and soaked with 1X transfer buffer in a container.

F.6 After running, the gels were soaked with 1X transfer buffer for 10-15 minutes.

F.7 Transfer apparatus were prepared;

a. Firstly, sandwich system was set. Sponge was placed on black side

b. One piece of Whatmann paper was placed on the sponge

c. Gel was placed on the Whatmann paper

d. Membrane was placed carefully onto the gel. Membrane must cover the gel properly. Air bubbles must be removed by using the roller

e. Then, again another piece of Whatmann paper was placed on the membrane

f. Another sponge was placed on Whatmann paper.

g. Finally, sandwich system was locked without displacing the system. All materials were immersed with transfer buffer.

F.8 Sandwich system was placed into the casette system and the casette was placed in the container. The container was filled with 1X transfer buffer until the buffer reached the top of the sandwich system.

F.9 Transfer was run at 100 mA for 2 hours at room temperature.

F.10 Blocking solution was prepared as 3% BSA with 0.05% T-TBS. After transfer, both membranes were soaked with blocking solution for 1 hour at room temperature. Membranes were put on shaker.

F.11 Primary Antibody solutions were prepared in 10 ml 3% BSA with 0.05% T-TBS. To make 1/1000 dilutions, 10 µl of Phospho-ERK1/2 antibody was mixed with this solution. Membranes were incubated with Primary antibody overnight at 4°C.

F.12 The primary antibody was discarded and membranes were washed three times, each 10 minutes at room temperature on shaker.

F.13 Secondary Antibody solution was prepared in 10 ml 3% BSA with 0.05 % T-TBS. To make 1/2000 dilutions, 5 µl of Anti- Rabbit IgG antibody was mixed with this solution. Membranes were incubated with Secondary Antibody for 1 hour at room temperature on the shaker

F.14 Secondary antibody was discarded and membranes were washed for three times, each 10 minutes at room temperature on the shaker

F.15 ECL solution was prepared. 1 unit A solution was mixed with 1 unit B solution. Membranes were covered with ECL solution for 1 minute in the dark room. The membranes were then placed in Saran wrap and most of the solution was removed from the Saran wrap using tweezers. Membranes were visualized using the UV transilluminator for 60 seconds to 120 seconds for the best image.

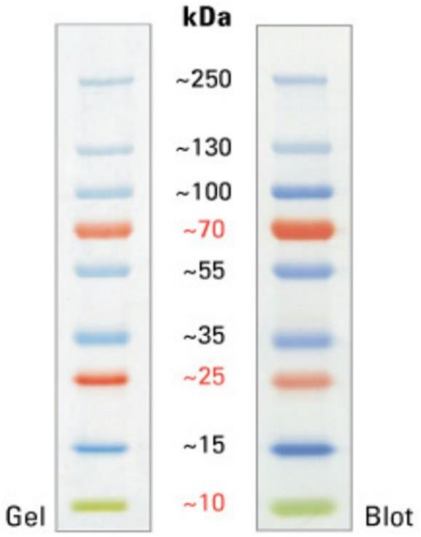

Figure F.1: Protein Ladder PageRuler Plus Prestained Protein Ladder 10 to 250 kDa

G. VERIFICATION OF 7 CANDIDATE CART RECEPTOR GENES IN TANGO VECTORS

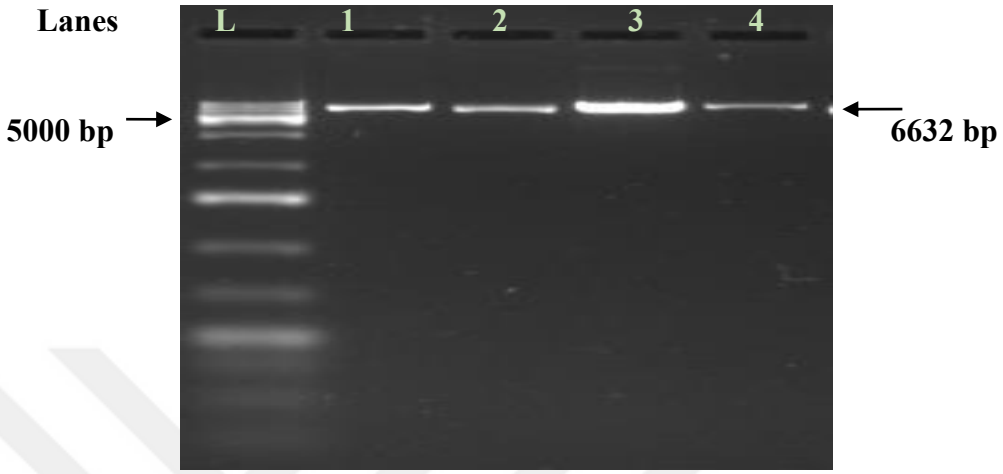

Figure G.1: Agarose Gel Image of Digested *GPR116* and *SCTR*. Ladder: (L): O'GeneRuler 1 kb Plus DNA Ladder. Lane 1 and 2: *GPR116* (old), Lane 3 and 4: *SCTR* (old). Genes were digested with 5 µl of NotI enzyme.

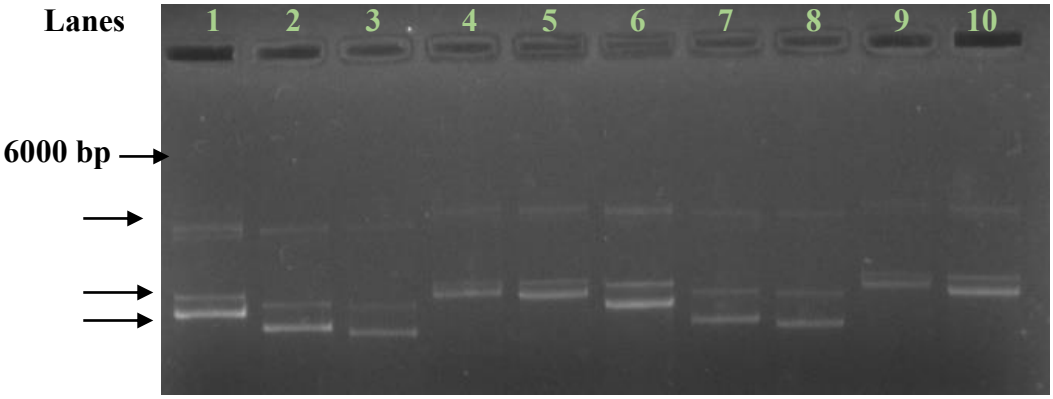

Figure G.2: Agarose Gel Image of Digested GPR133, GPR2R, GPR1R, GRM1 and CASR Plasmid DNAs. Lane 1: GPR133 (old), Lane 2: GLP2R (old), Lane 3: GLP1R (old), Lane 4: GRM1 (old), Lane 5: CASR (old), Lane 6: GPR133 (new), Lane 7: GLP2R (new), Lane 8: GLP1R (new), Lane 9: GRM1 (new), Lane 10: CASR (new), Genes were digested with 5 µl NotI enzyme.

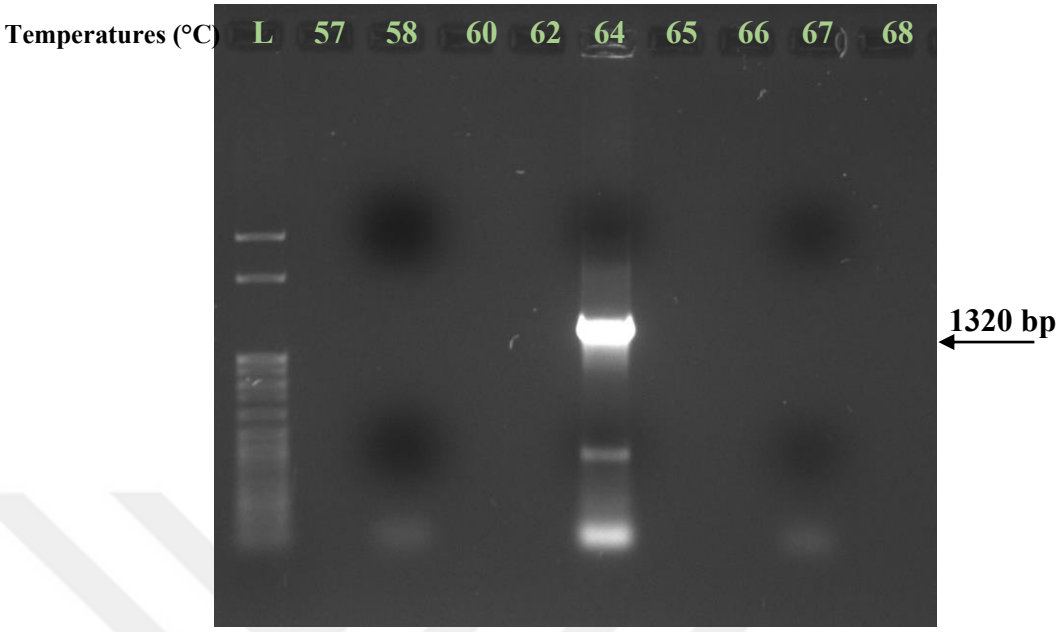

Figure G.3: Agarose Gel Image of Gradient PCR for Old *SCTR*. Amplification of *SCTR* was achieved at 64°C of annealing temperature. Left side indicates ladder. Ladder (L): Direct Load™ 50 bp DNA Step Ladder.

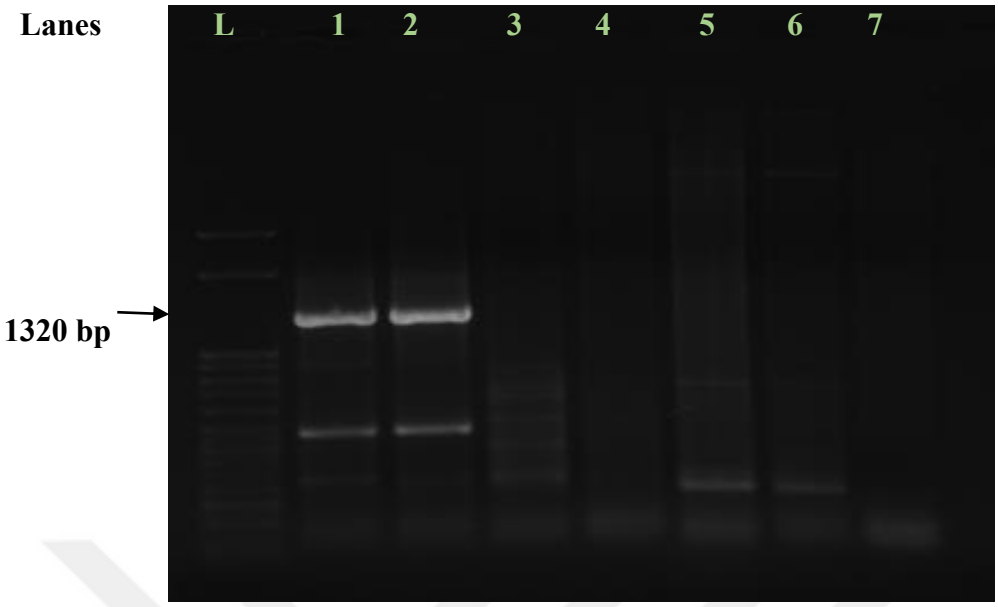

Figure G.4: Agarose Gel Image of PCR Product for the Old and New *SCTR*. (Lane 1: *SCTR1* from old plates (positive control) (old plasmids), Lane 2: *SCTR2* (old plasmids) (positive control), Lane 3: *SCTR* (new plasmids), Lane 4: *SCTR4* (new plasmids), Lane 5: *SCTR5* (new plasmids), Lane 6: *SCTR6* (new plasmids), Lane 7: Negative control (no DNA), Ladder (L): DirectLoad^{TM} 50 bp DNA Step Ladder.

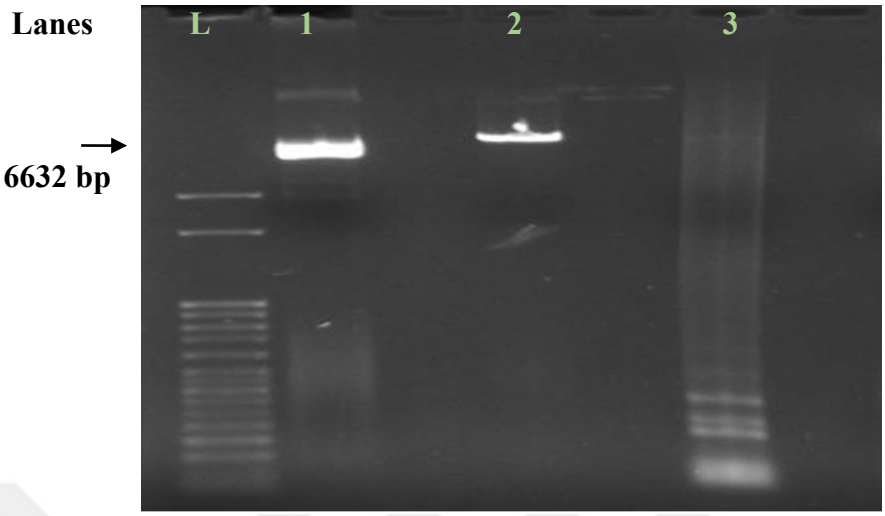

Figure G.5: Agarose Gel Image of New SCTR and its PCR Product. All these genes were analyzed in one gel. Ladder (L): DirectLoad^{TM} 50 bp DNA Step Ladder. Lane 1: Undigested *SCTR*, Lane 2: NotI Digested *SCTR*, Lane 3: PCR Product of digested *SCTR* (new SCTR genes were used).

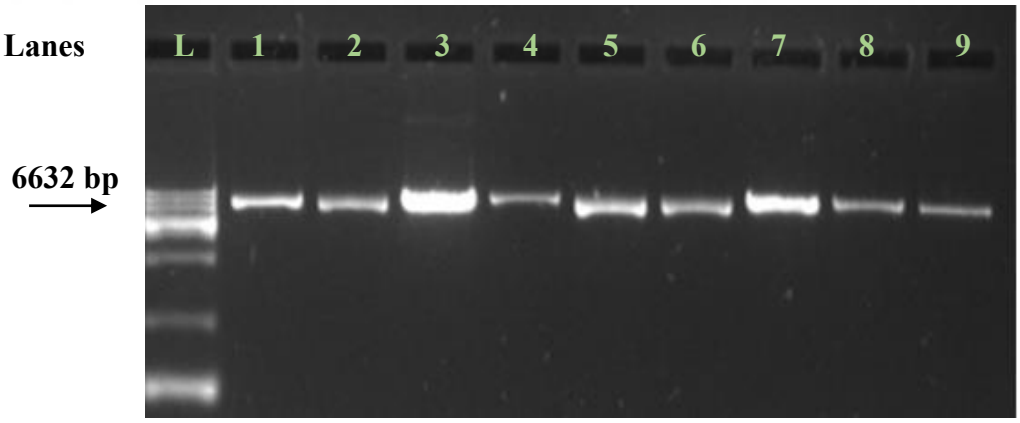

Figure G.6: Agarose Gel Image of 1.Part Plasmids. Gene sizes are almost 6500-8000 bp. Lane 1: *CASR*, Lane 2: *SCTR*, Lane 3: *CASR*, Lane 4: *GPR116*, Lane 5, 6: *SCTR*, Lane 7: *CASR*, Lane 8, 9: *GPR116*. Reference size: (R): O'GeneRuler 1 kb Plus DNA Ladder.

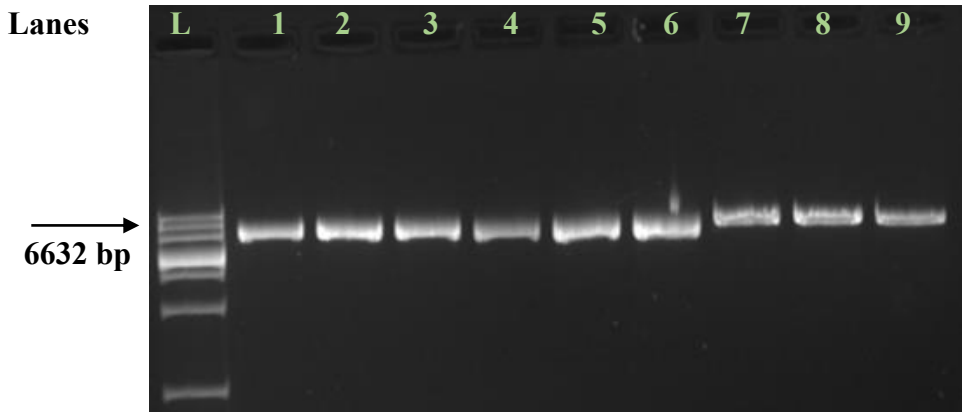

Figure G.7: Agarose Gel Image of 2. Part Plasmids (Gene sizes are almost 6500-8000 bp) Lane 1, 2, 3: *GLP2R*, Lane 4, 5, 6: *GLP1R*, Lane 7, 8, 9: *GRM1*. Reference size: (R): O'GeneRuler 1 kb Plus DNA Ladder.

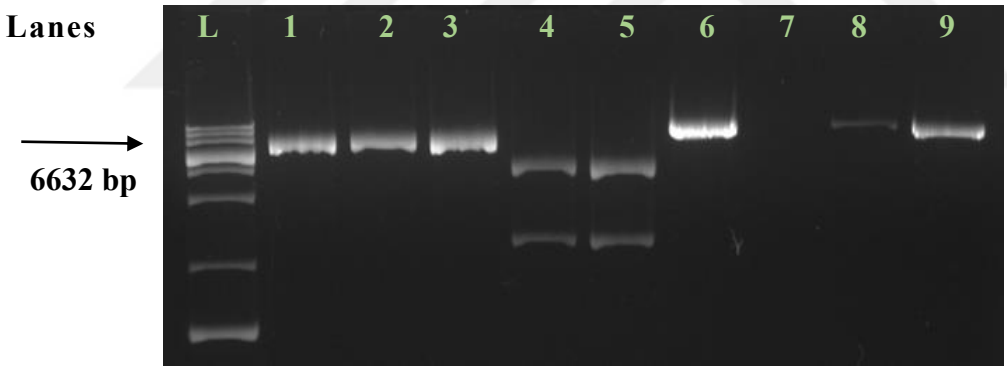

Figure G.8: Agarose Gel Image of 3. PART Plasmids (Gene sizes are almost 6500-8000 bp) Lane 1, 2, 3: *SCTR* (old plasmid), Lane 4, 5, 6: *CRHR1* (old plasmid), Lane 7, 8, 9: *GPR133*. Reference size (R): O'GeneRuler 1 kb Plus DNA Ladder.

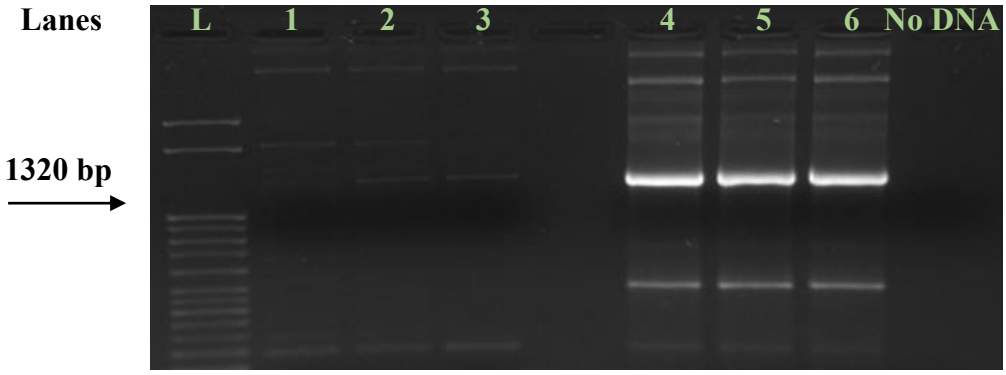

Figure G.9: Agarose Gel Image of PCR Products of New *SCTR*. *SCTR*: 1320 bp. Lane 1, 2, 3: *SCTR* (new plasmids), Lane 4, 5, 6: *SCTR* (old plasmids). Ladder (L): DirectLoad™ 50 bp DNA Step Ladder.

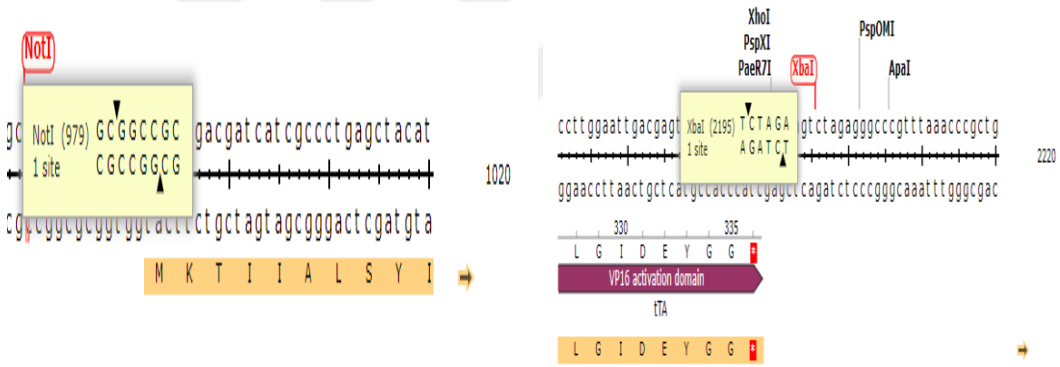

Figure G.10: Gene Range for *SCTR* by ADDGENE. Beginning and final sequences of the *SCTR* on the TANGO vector. This figure was reference sequence for *SCTR* from the ADDGENE website. The SCTR gene (1320 bp) was expected to be within the range of 979th to 2299th sequences.

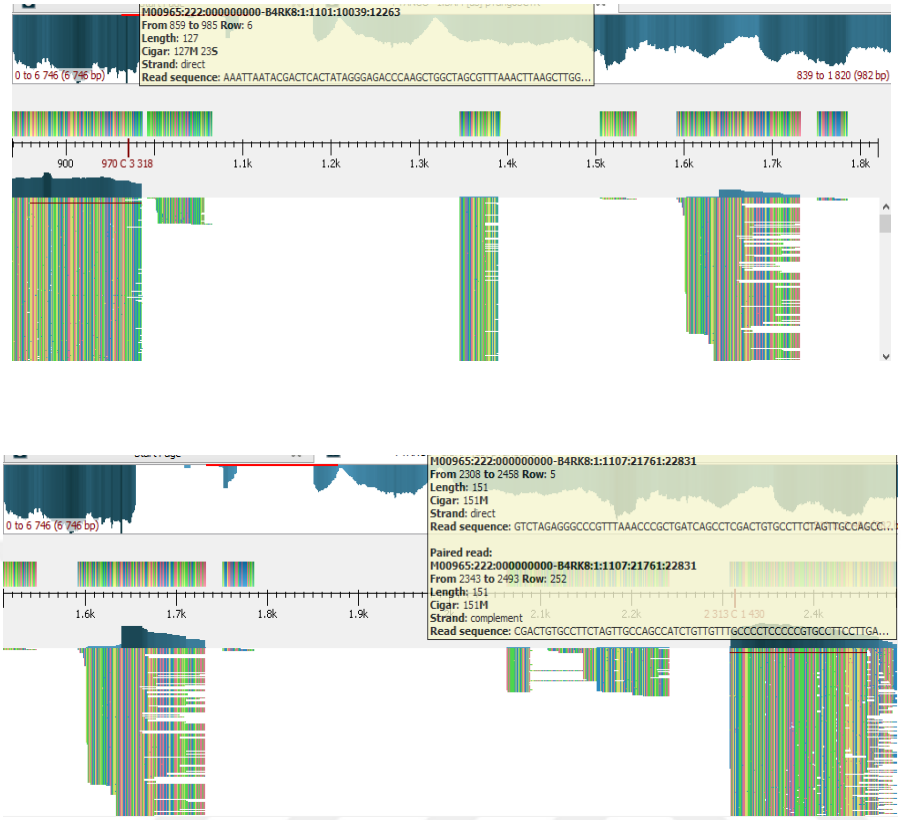

Figure G.11: UGENE Results. From 979th to 2458th sequence, there were no other sequences in the TANGO vector.

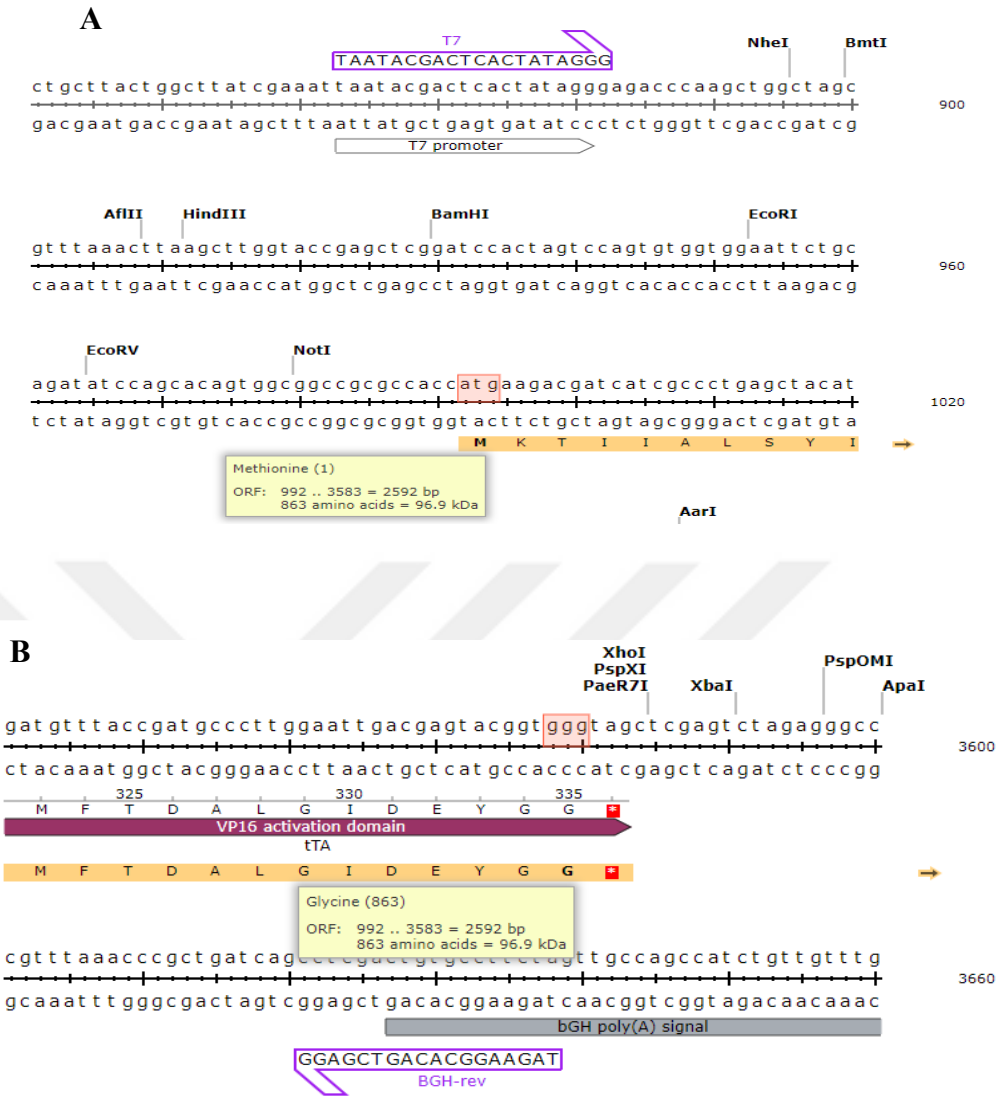

Figure G.12: The Gene Range of *GLP1R* and *GLP2R*. A. Beginning sequences of *GLP1R*, *GLP2R* and the open reading frame (ORF). *GLP1R* and *GLP2R* starts at 992th (colored by orange). **B.** Final sequences of the ORF that contains *TetR* (tetracycline controlled transactivator) in the TANGO vector that runs through 3583th sequence. *GLP1R* is between 992th and 2381th sequences which is total of 1389 bp. GLP2R is between 992th and 2651th sequences which is total of 1659 bp.

T7 Forward Primer

atgaagacgatcatcgccctgagctacatcttctgcctggtattcgccgactacaaggacgatgatgacgccagcatcgat
atggcaggtgcccctggacccctcaggctcgcactgctgcttctggggatggtcggacgagccggacccagacctcag
ggcgctaccgtgagtctttgggagaccgtccagaagtggcgggagtatcgccgccagtgtcaacgcagcctgacagaa
gatcctcctccagccaccgacttgttttgcaataggacatttgatgagtatgcctgctggccagacggcgagcccggctca
ttcgtgaatgtgtcatgtccatggtacctgccatgggcatcatctgtgcctcaaggacacgtctacaggttctgcacagctg
agggcctctggctgcaaaaagataacagttcccttccatggcgcgatcttagcgagtgcgaggaatctaagaggggcga
gcgcagttcccccgaggaacagctgctgtttctgtacattatctacaccgtcggctacgcgctgtccttttccgctctggttat
cgctagtgccatccttttggggtttcgccaccttcactgcacaagaaattacatccacttgaatctctttgcaagttttattctgc
gggccttgagtgtgttcattaaggacgctgccctgaagtggatgtactctaccgcggcccaacagcaccaatgggatgga
ctcctcagctatcaggattctctttcctgtcgactcgtgtttctgcttatgcagtactgtgtggcagccaattattattggctgct
ggtcgaaggagtatatctttacacactgctcgcattctccgtgctgagtgaacagtggattttcaggctttacgtgtccattgg
atggggtgtgcctctgctgttcgtggtgccttggggcatcgtcaagtacctgtatgaagatgaaggctgttggaccagaaa
ctctaacatgaactactggctcatcatacgcctgcccatactcttcgcgattggagtcaactttcttatatttgtgagagtgatc
tgtatcgtcgtgtcaaagctgaaagctaaccttatgtgcaaaaccgacattaagtgcagactggctaagtccactctcaccc
tcatcccgctgctcggaacacatgaagtgatatttgccttcgtgatggacgagcatgcgagaggcacactgcggtttatca
aactgttcacagagctgtctttcactagtttccaaggattgatggtggctattctctactgcttcgtgaacaatgaggtccaact
tgaatttcggaagtcatgggaacggtggcggcttgaacacctccatattcagcgcgatagttctatgaagccacttaaatgt
cccacttccagcctgagttccggagccaccgccggctcttcaatgtatacagccacttgtcaggcgtcctgctctatcgata
ccggtggacgcaccccacccagcctgggtccccaagatgagtcctgcaccaccgccagctcctccctggccaaggac
acttcatcgaccggtgagaacctgtacttccagctaagattagataaaagtaaagtgattaacagcgcattagagctgctta
atgaggtcggaatcgaaggtttaacaacccgtaaactcgcccagaagctaggtgtagagcagcctacattgtattggcat
gtaaaaaataagcgggctttgctcgacgccttagccattgagatgttagataggcaccatactcacttttgccctttagaagg
ggaaagctggcaagatttttacgtaataacgctaaaagttttagatgtgctttactaagtcatcgcgatggagcaaaagtac
atttaggtacacggcctacagaaaaacagtatgaaactctcgaaaatcaattagccttttatgccaacaaggtttttcactag
agaatgcattatatgcactcagcgctgtggggcattttactttaggttgcgtattggaagatcaagagcatcaagtcgctaaa
gaagaaagggaaacacctactactgatagtatgccgccattattacgacaagctatcgaattatttgatcaccaaggtgca
gagccagccttcttattcggccttgaattgatcatatgcggattagaaaaacaacttaaatgtgaaagtgggtccgcgtaca
gccgcgcgcgtacgaaaaacaattacgggtctaccatcgagggcctgctcgatctcccggacgacgacgcccccgaa

gaggcggggctggcggctccgcgcctgtcctttctccccgcgggacacacgcgcagactgtcgacggcccccccgac
cgatgtcagcctgggggacgagctccacttagacggcgaggacgtggcgatggcgcatgccgacgcgctagacgattt
cgatctggacatgttgggggacggggattccccgggtccgggatttaccccccacgactccgccccctacggcgctctg
gatatggccgacttcgagtttgagcagatgtttaccgatgcccttggaattgacgagtacggtgggtag

BGH Reverse Primer

Figure G.13: Blastn of *GLP1R*. Sequences between the yellow colors indicate T7 forward primer reading. Sequences between purple colors indicate the designed primer reading (Table G.1) for *GLP1R*. Sequences between green colors indicate BGH reverse primer reading. Sequences between red colors indicate the *GLP1R* sequence (1389 bp). After the *GLP1R* sequence, *TetR* sequence was also read by Sanger sequencing. Blue color shows the stop codon. The total sequence between 992th to 3583th is 2591 bp which confirms PCR result for *GLP1R* as in Figure 9. It demonstrated that the GLP1R gene is present in the TANGO vector.

Table G.1: Forward Primer Sequence for *GLP1R*

Forward Primer Sequence:
ACCAATGGGATGGACTCCTCAG

T7 Forward Primer

atgaaactcgggtcttccagggccggaccagggaggggctccgctggtctcctgcccggcgtacacgaactgccaatg
ggaatcccagctccctgggggaccagtcctctcagcttccacaggaaatgttctctgtgggctccgggccgcccgttcctt
acactggtattgcttgtgtctattaaacaggtcacaggctcattgctggaggaaaccacaagaaaatgggcgcagtacaa
gcaggcctgcctgcgcgacctgctgaaagaaccttcagggatttttgtaacggcacgtttgaccagtacgtctgctggcc
tcatagttctcctgggaacgttagtgtgccctgtccttcttatctgccctggtggtctgaggagtcttctgggagagcctacc
ggcactgcctggcacagggcacttggcagactattgagaatgctaccgacatctggcaggatgattctgagtgtagcga
gaaccacagctttaagcagaatgtcgatcgctatgccctgctgtccacacttcagcttatgtacacagtgggttactcattct
ccctgatcagcttgttccttgcgctgaccctgctccttttttcttagaaagctgcattgtacacggaactatattcatatgaatctg
tttgcaagcttcatactcaggaccttggcggtgctcgtcaaagatgtggtgttctacaatagttactccaagcggcctgaca
atgagaacggatggatgtcatacctgtctgaaatgtcaactagctgccgctcagtccaggtcctgcttcattattttgttggc
gccaactatctgtggctgctggttgaggggctctatcttcataccctgctggagccaactgttctcccggagcgccgcctgt
ggccacgatacttgttgctgggatgggcttttcctgtgctgtttgtggtgccttggggattcgcaagggctcaccttgagaac
actggttgctggactactaatgggaataaaaagatttggtggataatccggggccctatgatgctgtgtgtgaccgtcaact
tttttatcttcctcaaaattctgaaactcctcatctccaagctgaaagcccaccagatgtgctttcgcgattataagtataggttg
gcaaagtcaacattggttcttatccctttgttgggagtccatgaaatcttgttctcatttattacagacgatcaggtggagggat
tcgcaaagctgatccgactctttatccagctgactctgtctagcttccatggattcctcgtggccctgcagtacggcttcgct
aatggagaggtgaaggccgagcttagaaagtactgggtacgctttctgcttgcacggcactccgggtgcagagcgtgcg
tcctgggaaaggacttcagatttctggggaaatgcccaaagaagctgtccgaaggggacggcgctgaaaagcttagaa
agcttcaaccatccctgaactctggccgactgcttcatctggccatgcggggcctgggggagctgggtgcgcagccaca
gcaggaccacgcgcgctggcctagaggcagtagcctttcagagtgtagtgaaggtgacgttaccatggcaaatacaatg
gaggaaattctcgaagagtcagagatcagattagataaaagtaaagtgattaacagcgcattagagctgcttaatgaggtc
ggaatcgaaggtttaacaacccgtaaactcgcccagaagctaggtgtagagcagcctacattgtattggcatgtaaaaaat
aagcgggctttgctcgacgccttagccattgagatgttagataggcaccatactcacttttgccctttagaaggggaaagct
ggcaagatttttacgtaataacgctaaaagttttagatgtgctttactaagtcatcgcgatggagcaaaagtacatttaggta
cacggcctacagaaaaacagtatgaaactctcgaaaatcaattagccttttttatgccaacaaggtttttcactagagaatgca
ttatatgcactcagcgctgtggggcattttactttaggttgcgtattggaagatcaagagcatcaagtcgctaaagaagaaa
gggaaacacctactactgatagtatgccgccattattacgacaagctatcgaattatttgatcaccaaggtgcagagccag
ccttcttattcggccttgaattgatcatatgcggattagaaaaacaacttaaatgtgaaagtgggtccgcgtacagccgcgc

gcgtacgaaaaacaattacgggtctaccatcgagggcctgctcgatctcccggacgacgacgcccccgaagaggcgg
ggctggcggctccgcgcctgtcctttctccccgcgggacacacgcgcagactgtcgacggcccccccgaccgatgtca
gcctgggggacgagctccacttagacggcgaggacgtggcgatggcgcatgccgacgcgctagacgatttcgatctg
gacatgttgggggacggggattccccgggtccgggatttacccccccacgactccgcccccctacggcgctctggatatgg
ccgacttcgagtttgagcagatgtttaccgatgcccttggaattgacgagtacggtgggtag

BGH Reverse Primer

Figure G.14: Blastn of *GLP2R*. Sequences between the yellow colors indicate T7 forward primer reading. Sequences between purple colors indicate the designed primer reading (Table G.2) for *GLP2R*. Sequences between green colors indicate BGH reverse primer reading. Sequences between red colors indicate the *GLP2R* sequence (1659 bp). After the *GLP2R* sequence, *TetR* sequence was also read by Sanger sequencing. Blue color shows the stop codon. The total sequence is 2661 bp which confirms PCR result for *GLP2R* as in Figure 9. The vector contains *GLP2R*.

Table G.2: Forward Primer Sequence for *GLP2R*

Forward Primer Sequence:
TCTGAAATGTCAACTAGCTGC